

Sizing Grid-Connected Wind Power Generation and Energy Storage Considering Wake Effect and Endogenous Uncertainty: A Distributionally Robust Method

Rui Xie^a, Wei Wei^b, Yue Chen^{a,*}

^a*Department of Mechanical and Automation Engineering, the Chinese University of Hong Kong, Hong Kong SAR.*

^b*State Key Laboratory of Power Systems, Department of Electrical Engineering, Tsinghua University, Beijing 100084, China.*

Abstract

Wind power, as a green energy resource, is growing rapidly worldwide, along with energy storage systems (ESSs) to mitigate its volatility. Sizing of wind power generation and ESSs has become an important problem to be addressed. Wake effect in a wind farm can cause wind speed deficits and a drop in downstream wind turbine power generation, which however was rarely considered in the sizing problem in power systems. In this paper, a bi-objective distributionally robust optimization (DRO) model is proposed to determine the capacities of wind power generation and ESSs considering the wake effect. An ambiguity set based on Wasserstein metric is established to characterize the wind power and demand uncertainties. In particular, wind power uncertainty is affected by the wind power generation capacity which is determined in the first stage. Thus, the proposed model is a DRO with endogenous uncertainty (or decision-dependent uncertainty). To solve the proposed model, a stochastic programming approximation method based on minimum Lipschitz constants is developed to turn the DRO model into a linear program. Then, an iterative algorithm is built, embedded with methods for evaluating the minimum Lipschitz constants. Case studies demonstrate the necessity of considering wake effect and the effectiveness of the proposed method.

Keywords: sizing, wake effect, endogenous uncertainty, distributionally robust optimization, energy storage

Nomenclature

Abbreviations

DDU	Decision-dependent uncertainty.
DRO	Distributionally robust optimization.
ESS	Energy storage system.
RO	Robust optimization.
SP	Stochastic programming.
WT	Wind turbine.

Indices and Sets

$i \in S^B$	Set of buses.
$(i, j) \in S^L$	Set of transmission lines.
$t \in S^T$	Set of periods.
$n \in S^E$	Set of extreme scenarios.
$n \in S^N$	Set of normal scenarios.

*Corresponding author

Email address: yuechen@mae.cuhk.edu.hk (Yue Chen)

Parameters

Δ_t	Period length.
$b_{i,k}^{(1)}, b_{i,k}^{(2)}$	Coefficients of the fuel cost.
$\underline{P}_i^G, \overline{P}_i^G$	Lower and upper bounds for generation power of the traditional generator at bus i .
$\underline{R}_i^G, \overline{R}_i^G$	Lower and upper bounds for the ramp rate of the traditional generator at bus i .
η^{SC}, η^{SD}	Charging and discharging efficiencies of the ESSs.
$\underline{\omega}^S, \overline{\omega}^S$	Lower and upper bounds for state-of-charge of the ESSs.
X_{ij}^L	Reactance of the transmission line from bus i to bus j .
S_{ij}^L	Capacity of the transmission line from bus i to bus j .
$\varepsilon^E, \varepsilon^N$	Size parameters of the ambiguity sets in extreme and normal conditions.
C_i^W	Unit capacity cost of the wind farm at bus i .
C^{SP}, C^{SE}	Unit costs of ESS power and energy capacities.
\overline{g}^E	Maximum acceptable load shedding expectation in extreme conditions.

Uncertain Variables and Decision Variables

$\zeta_{i,t}^D$	Uncertain variable of load demand at bus i in period t .
$\xi_{i,t}^W$	Uncertain and auxiliary variable representing the wind condition of wind farm at bus i in period t .
$\zeta_{i,t}^W$	Decision-dependent uncertain variable of power generation of the wind farm at bus i in period t .
$p_{i,t}^C$	Power curtailment at bus i in period t .
$p_{i,t}^D$	Load shedding power at bus i in period t .
$p_{i,t}^G$	Power generation of the traditional generator at bus i in period t .
$f_{i,t}^G$	Fuel cost of the traditional generator at bus i in period t .
$p_{i,t}^{SC}, p_{i,t}^{SD}$	Charging power and discharging power of the ESS at bus i in period t .
$e_{i,t}^S$	Stored energy of the ESS at bus i in the end of period t .
$p_{ij,t}^L$	Active power flow of the transmission line from bus i to bus j in period t .
$\theta_{i,t}^B$	Voltage angle at bus i in period t .
x_i^{SP}, x_i^{SE}	Investment variables of power capacity and energy capacity of the ESS at bus i .
x_i^W	Investment variable of power capacity of the wind farm at bus i .

1. Introduction

The large-scale integration of renewable energy is one of the worldwide efforts towards carbon neutrality [1]. Wind power, as one of the leading clean energy resources, has developed rapidly in recent years. However, wind resources are affected by weather conditions, leading to highly volatile and stochastic wind power, which threatens the power system operation. Energy storage systems (ESSs) that can shift energy over time are installed to better accommodate uncertain renewable generations. Therefore, the sizing of wind power generation and ESSs is an important problem to be addressed.

A vast literature has been devoted to the generation and ESS siting and sizing problems in renewable-integrated power systems. These studies can be divided into three categories based on stochastic programming (SP), robust optimization (RO), and distributionally robust optimization (DRO), respectively. The SP methods assume known probability distributions of the uncertainties, which are represented either by parametrized distributions or a set of scenarios. The sizing problem of generation and storage expansion [2], ESS capacities considering frequency dynamics constraints [3], and shared ESS for 5G base stations [4] were

studied using the SP method. In [5], the reduction of wind power prediction error caused by the aggregation effect was modeled by decision-dependent Gaussian distributions and further represented by generated scenarios. However, in practice, it is difficult to obtain the accurate uncertainty distribution in the planning stage, and an inexact empirical distribution may lead to infeasible or suboptimal results. To overcome this shortcoming, RO has been adopted, which optimizes the performance under the worst-case scenario within an uncertainty set. A multi-objective robust model was proposed for ESS allocation [6], where the uncertain demands and renewable generation were modeled. Apart from the short-term fluctuations, reference [7] further considered the long-term uncertainties of load and renewable growths in the ESS planning problem. However, as the worst case rarely happens, the RO method may lead to over-conservative sizing results.

DRO technique is in-between SP and RO methods, which optimizes decisions with respect to the worst-case distribution in a predefined ambiguity set. It can achieve a good tradeoff between optimality and robustness. DRO method has appeared in power system operation problems. Unimodality and moment were used in [8] to construct the ambiguity set for distributionally robust optimal power flow (OPF). Wasserstein-metric-based ambiguity sets were used in [9] and [10] for OPF in power systems and optimal dispatch in integrated electricity and heat systems, respectively. DRO method has also been adopted in power system sizing problems. Aiming at optimal generation expansion, a DRO model with risk constraints was put forward in [11] with an ambiguity set based on moments and unimodality. However, large numbers of data are needed to accurately estimate moments and different distributions may have the same moments. A DRO siting and sizing method for ESS was proposed in [12] based on Kullback-Leibler divergence, where the ESS lifespan model was considered. However, such divergence is only well-defined for discrete distributions supported on the range of the sample data. On the contrary, Wasserstein distance is able to measure the difference between general distributions. A distributionally robust chance-constrained model was proposed for clustered generation expansion in [13] with a Wasserstein-metric-based ambiguity set. However, none of the studies above considered the wake effect in a wind farm.

The wake effect in a wind farm refers to the decrease in gross energy production due to the changes in wind speed caused by the impact of wind turbines (WTs) on each other. To be specific, the wake from the upstream WTs decreases the wind's kinetic energy and lowers the wind speed at the downstream WTs. Studies on wind farms have been aware of the wake effect and considered it in problems such as reliability evaluation [14], dynamic equivalent model [15], control strategy [16], maintenance scheduling [17], etc. As the wake effect can reduce the power output by about 20% [18], it is nonnegligible in wind farm planning. Currently, the wake effect is mainly considered in the layout design of wind farms. For instance, the inter-array layout planning in an offshore wind farm was optimized in [19] using particle swarm optimization. Another layout optimization approach was proposed in [20] based on an adaptive evolutionary algorithm with Monte Carlo tree search reinforcement learning. The comprehensive problem of wind farm area, shape, and layout decisions was studied in [21] and the method was applied to an offshore wind farm in the UK. The optimal ESS allocation inside the wind farm was investigated in [22] to better support frequency. However, the aforementioned studies did not consider the impact of wind power generation on power system operation. The SP method proposed in [23] planned wind farms in distribution systems, where the wake effect was integrated via simulations. The optimal solution was searched in an enumeration manner with an acceleration constraint, which may be computationally expensive for bulk power systems with a large number of WTs.

This paper proposes a distributionally robust optimization method with a decision-dependent ambiguity set for sizing wind power generation and energy storage considering the wake effect. The contributions are:

(1) **Sizing Model.** A distributionally robust optimization model is developed for the sizing of wind power generation and ESSs in power systems. The worst-case expected fuel cost in normal operation conditions is minimized while the worst-case expected load shedding in extreme conditions is upper bounded in the constraint. Distinct from the traditional models, the wake effect in a wind farm is considered. This makes the sizing model more practical. In particular, simulations are carried out to evaluate the wake effect. Based on this, a piecewise linear model showing how the available wind power generation changes with wind

conditions and the capacity is developed. The model is then used for modeling wind power uncertainty via Wasserstein-metric-based ambiguity sets. Due to the wake effect, the size of the ambiguity set depends on the first-stage sizing decisions, and is thus decision-dependent. Therefore, the proposed model is a DRO problem with both endogenous/decision-dependent uncertainty (DDU) and exogenous/decision-independent uncertainty (DIU).

(2) **Solution Method.** To solve the proposed model, we first develop an SP approximation of it with the help of minimum Lipschitz constants. Then, an iterative algorithm embedded with methods for calculating the upper bounds of the minimum Lipschitz constants is established to solve the obtained SP problem. The proposed algorithm is novel in that it provides a systematic method for solving the Wasserstein-metric-based DRO model and can deal with DDUs that are seldom considered in previous work.

The rest of this paper is organized as follows. Section 2 establishes a linear approximation of available wind power function considering the wake effect. A distributionally robust wind-storage sizing model that takes into account the wake effect is proposed in Section 3 with solution method developed in Section 4. Case studies are reported in Section 5. Finally, Section 6 concludes the paper.

2. Linearized Available Wind Power Function Considering Wake Effect

In this section, we characterize the available wind power in a wind farm considering the wake effect. First, the Jensen wake model is adopted to model the wake effect of a single WT. Simulations are carried out to calculate the available wind power in a wind farm under different total WT capacities and real-time wind conditions, whose relationship is a nonlinear function. Then, the nonlinear function is further linearized for computational tractability.

2.1. Available Wind Power By Simulation

Jensen wake model is a widely used analytical wake model [24]. Suppose the wind direction is parallel to the line between two WTs, then according to the Jensen wake model, the wind speed at the downstream WT can be calculated as follows [25]:

$$v_2^W = v_1^W \left(1 - \left(1 - \sqrt{1 - C^T} \right) \left(\frac{D^R}{D^R + 2K^W d^W} \right)^2 \right), \quad (1)$$

$$K^W = 0.5 / \ln(H^H / Z^R), \quad (2)$$

where v_1^W and v_2^W are the wind speed values at the upstream and downstream WTs, respectively; d^W is the distance between the two WTs; the thrust factor C^T , the turbine rotor diameter D^R , the hub height H^H , and the roughness length Z^R are parameters; K^W is the wake decay constant. As (1) shows, the closer the two WTs to each other, the stronger the wake and the wind speed deficit.

For simplicity, we consider the wind farm layout in Figure 1 as an example: The wind farm will be built in a given rectangular area; all WTs have the same types and parameters and are placed evenly; the wind is blowing parallel to the rows of WTs; the distance between adjacent rows is fixed and large enough so that the wake effect between rows can be neglected. A similar assumption can be found in [25]. Nonetheless, other wind farm layouts as well as wake models can be used for simulation and the subsequent process from Section 2.2 to Section 4 can still be carried out. Suppose the length of a row is R^P and the number of WTs in a row is $n^W > 1$, then the distance between adjacent WTs is $d^W = R^P / (n^W - 1)$. The wind speed at the i -th WT is

$$v_i^W = v_1^W \left(1 - \left(1 - \sqrt{1 - C^T} \right) \left(\frac{D^R}{D^R + 2K^W d^W} \right)^2 \right)^{i-1}. \quad (3)$$

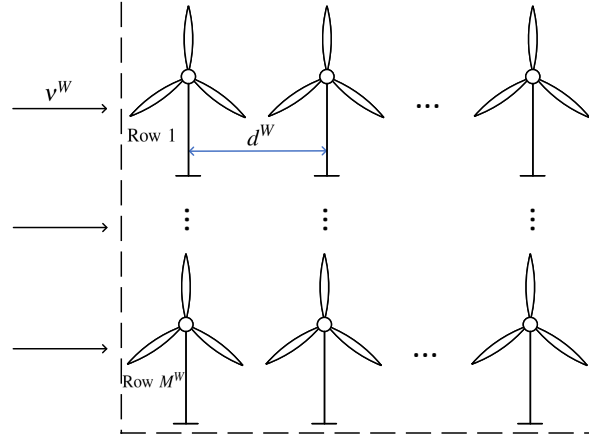


Figure 1: Wind farm layout as an example.

The available wind power of one WT can be calculated using the following function [26].

$$p^W(v) := \begin{cases} 0, & \text{if } v \leq V^C \text{ or } v > V^F, \\ P^R \frac{v^2 - (V^C)^2}{(V^R)^2 - (V^C)^2}, & \text{if } V^C < v \leq V^R, \\ P^R, & \text{if } V^R < v \leq V^F, \end{cases} \quad (4)$$

where p^W is the available wind power and v is the wind speed at this WT; the cut-in speed V^C , cut-out speed V^F , rated speed V^R , and rated power P^R are parameters. Sum up the available power of all WTs, then we have the available wind power of the wind farm $f^W := M^W \sum_{i=1}^{n^W} p^W(v_i^W)$, where M^W is the number of rows. Given n^W and the initial wind speed $v^W := v_1^W$ at the wind farm, the total capacity of WTs $x^W = P^R M^W n^W$ and the total available wind power f^W can be uniquely determined. Hence, we can characterize the change of available wind power with x^W and v^W by simulations.

To be specific, let \bar{n}^W and \bar{v}^W denote the upper bounds of n^W and v^W , respectively. Use $N^V + 1$ wind speed values for discretization. For $n^W = 1, 2, \dots, \bar{n}^W$ and $v^W = 0, \bar{v}^W/N^V, 2\bar{v}^W/N^V, \dots, \bar{v}^W$, calculate the corresponding f^W and x^W and get tuples (x_l^W, v_l^W, f_l^W) for $l = 1, 2, \dots, \bar{n}^W(N^V + 1)$. The change of f^W with x^W and v^W is shown in Figure 2 (left). When v^W is fixed, as x^W varies from 0 to $\bar{x}^W := P^R M^W \bar{n}^W$, f^W first increases proportionally, but then its growth slows down; f^W even decreases when x^W is too large because of the severe wake effect. This shows the necessity of considering the wake effect in the sizing problem.

2.2. Linearized Available Wind Power Function

Considering that the relationship between f^W and x^W, v^W is highly nonlinear, to facilitate the computation, we establish a piecewise linear approximation for the available wind power function. First, to eliminate the nonlinear term in (4), we introduce an auxiliary variable ξ^W as follows.

$$\xi^W(v^W) := \begin{cases} 0, & \text{if } v^W \leq V^C, \\ \frac{(v^W)^2 - (V^C)^2}{(V^R)^2 - (V^C)^2}, & \text{if } v^W > V^C. \end{cases} \quad (5)$$

Then, the available wind power f^W can be viewed as a function of x^W and ξ^W , which is depicted in Figure 2 (right). The actual wind power output can vary within 0 and f^W , so the feasible region of wind power is the region below the plane in Figure 2 and above zero, which can be approximated by its convex hull.

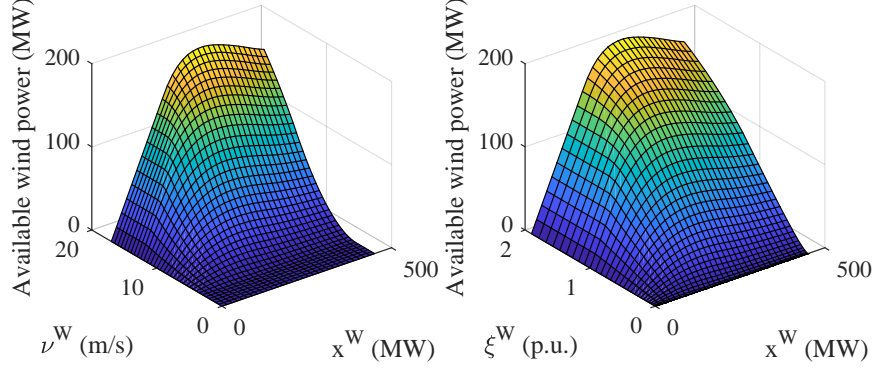


Figure 2: The change of available wind power f^W with the total capacity x^W and initial wind speed ν^W / auxiliary variable ξ^W .

Multi-Parametric Toolbox (MPT) 3.0 [27] can find the convex hull of a set of points, which is represented by its extreme point set or a linear inequality set describing the facets. We use MPT to find the convex hull of the feasible region of wind power and get a polyhedron as follows.

$$\mathcal{P}^W := \left\{ (x^W, \xi^W, p^W) \left| \begin{array}{l} p^W \geq 0, x^W \leq \bar{x}^W, \xi^W \leq \bar{\xi}^W \\ p^W \leq a_k^{(1)} x^W + a_k^{(2)} \xi^W + a_k^{(3)}, \forall k \in \mathcal{K}_0^a \end{array} \right. \right\}, \quad (6)$$

where $a_k^{(1)}$, $a_k^{(2)}$, and $a_k^{(3)}$ are the parameters of inequalities and $\min_{k \in \mathcal{K}_0^a} \{a_k^{(1)} x^W + a_k^{(2)} \xi^W + a_k^{(3)}\}$ is a piecewise linear approximation of the available wind power function.

There may be a large number of inequalities in (6). To improve the computational efficiency, we propose Algorithm 1 to select a representative subset of inequalities while maintaining acceptable precision. Algorithm 1 starts from a cuboid containing the original polyhedron, and adds the remaining most important inequality in each iteration until the approximation error is lower than a certain level. Algorithm 1 always converges because the number of inequalities is finite.

3. Distributionally Robust Sizing Model

In this section, we first propose models to evaluate the operation costs given the sizing strategies (capacities), and then build the ambiguity sets, based on which the distributionally robust sizing model is established.

3.1. Operation Problems

First, we consider the operation stage with given wind power generation and ESS capacities and uncertainty realizations. Two models are developed to evaluate the operation cost under 1) *normal conditions*, where the total fuel cost is minimized and load shedding is not allowed; and 2) *extreme conditions*, where the total load shedding is minimized.

3.1.1. Power System Operation Constraints

Let $S^T := \{1, 2, \dots, T\}$, S^B , and S^L be the set of periods, buses, and transmission lines, respectively. Denote the period length by Δ_t . The power system operation constraints are as follows.

$$f_{i,t}^G = \max_{k \in \mathcal{K}^b} \{b_{i,k}^{(1)} p_{i,t}^G \Delta_t + b_{i,k}^{(2)}\}, \forall i \in S^B, t \in S^T, \quad (7a)$$

$$\underline{p}_i^G \leq p_{i,t}^G \leq \bar{p}_i^G, \forall i \in S^B, t \in S^T, \quad (7b)$$

Algorithm 1: Selection of representative inequalities

Input: Error tolerance $\varepsilon > 0$, \bar{x}^W , $\bar{\xi}^W$, and inequality coefficients $(a_k^{(1)}, a_k^{(2)}, a_k^{(3)})$, $k \in \mathcal{K}_0^a$.

Output: A set $\mathcal{K}^a \subset \mathcal{K}_0^a$ and the approximate polyhedron \mathcal{P} .

- 1: Initiation: Let $\mathcal{K}^a \leftarrow \emptyset$.
- 2: Let the approximate polyhedron \mathcal{P} be

$$\left\{ (x^W, \xi^W, p^W) \left| \begin{array}{l} 0 \leq x^W \leq \bar{x}^W, 0 \leq \xi^W \leq \bar{\xi}^W \\ 0 \leq p^W \leq \bar{p}^W \\ p^W \leq a_k^{(1)} x^W + a_k^{(2)} \xi^W + a_k^{(3)}, \forall k \in \mathcal{K}^a \end{array} \right. \right\}.$$

- 3: Find the extreme points (x_l^W, ξ_l^W, p_l^W) , $l \in \mathcal{I}$ of \mathcal{P} via MPT, where \mathcal{I} is the index set.

- 4: Calculate the maximum approximation error

$$\max_{l \in \mathcal{I}} \left\{ \max_{k \in \mathcal{K}_0^a \setminus \mathcal{K}^a} \left\{ p_l^W - (a_k^{(1)} x_l^W + a_k^{(2)} \xi_l^W + a_k^{(3)}) \right\} \right\},$$

where the inside max calculates the approximation error at (x_l^W, ξ_l^W) . If the error is no larger than ε , terminate; otherwise, suppose $k_0 \in \mathcal{K}_0^a \setminus \mathcal{K}^a$ reaches the above maximum, then update $\mathcal{K}^a \leftarrow \mathcal{K}^a \cup \{k_0\}$ and go to Step 2.

$$\underline{R}_i^G \Delta_t \leq p_{i,t}^G - p_{i,t-1}^G \leq \bar{R}_i^G \Delta_t, \forall i \in \mathcal{S}^B, t \in \mathcal{S}^T \setminus \{1\}, \quad (7c)$$

$$\underline{R}_i^G \Delta_t \leq p_{i,1}^G - p_{i,T}^G \leq \bar{R}_i^G \Delta_t, \forall i \in \mathcal{S}^B, \quad (7d)$$

$$0 \leq p_{i,t}^{SC} \leq x_i^{SP}, 0 \leq p_{i,t}^{SD} \leq x_i^{SP}, \forall i \in \mathcal{S}^B, t \in \mathcal{S}^T, \quad (7e)$$

$$e_{i,t}^S = e_{i,t-1}^S + \left(\eta^{SC} p_{i,t}^{SC} - \frac{p_{i,t}^{SD}}{\eta^{SD}} \right) \Delta_t, \forall i \in \mathcal{S}^B, t \in \mathcal{S}^T \setminus \{1\}, \quad (7f)$$

$$e_{i,1}^S = e_{i,T}^S + \left(\eta^{SC} p_{i,1}^{SC} - \frac{p_{i,1}^{SD}}{\eta^{SD}} \right) \Delta_t, \forall i \in \mathcal{S}^B, \quad (7g)$$

$$\underline{\omega}^S x_i^{SE} \leq e_{i,t}^S \leq \bar{\omega}^S x_i^{SE}, \forall i \in \mathcal{S}^B, t \in \mathcal{S}^T, \quad (7h)$$

$$p_{ij,t}^L = \frac{\theta_{i,t}^B - \theta_{j,t}^B}{X_{ij}^L}, -S_{ij}^L \leq p_{ij,t}^L \leq S_{ij}^L, \forall (i,j) \in \mathcal{S}^L, t \in \mathcal{S}^T, \quad (7i)$$

$$0 \leq p_{i,t}^D \leq \zeta_{i,t}^D, p_{i,t}^C \geq 0, \forall i \in \mathcal{S}^B, t \in \mathcal{S}^T, \quad (7j)$$

$$\begin{aligned} & \sum_{(k,i) \in \mathcal{S}^L} p_{ki,t}^L + p_{i,t}^G + \zeta_{i,t}^W + p_{i,t}^{SD} - p_{i,t}^C \\ & = \sum_{(i,j) \in \mathcal{S}^L} p_{ij,t}^L + p_{i,t}^{SC} + \zeta_{i,t}^D - p_{i,t}^D, \forall i \in \mathcal{S}^B, t \in \mathcal{S}^T. \end{aligned} \quad (7k)$$

Constraints (7a)-(7d) constitute the model of traditional generators, where $p_{i,t}^G$ and $f_{i,t}^G$ denote the generation power and fuel cost of the traditional generator at bus i in period t , respectively. The fuel cost is modeled by the maximum of a set of linear functions in (7a), where $b_{i,k}^{(1)}, b_{i,k}^{(2)}, k \in \mathcal{K}^b$ are constant coefficients. Constraint (7b) stipulates the range $[P_i^G, \bar{P}_i^G]$ of generation power. Constraints (7c) and (7d) consist of the lower bound \underline{R}_i^G and upper bound \bar{R}_i^G of ramp rates, where (7d) ensures continuous operation. Constraints (7e)-(7h) compose the model of ESSs, where $p_{i,t}^{SC}$, $p_{i,t}^{SD}$ are the charging and discharging power of the ESS at bus i in

period t , respectively; $e_{i,t}^S$ is the stored energy at the end of period t . The power and energy capacities of the ESS at bus i are denoted by x_i^{SP} and x_i^{SE} , respectively. Constraint (7e) limits the charging/discharging power. Constraints (7f) and (7g) are for the dynamics of the stored energy, with charging and discharging efficiencies η^{SC} and η^{SD} . Constraint (7h) stipulates the lower bound $\underline{\omega}^S$ and upper bound $\bar{\omega}^S$ of ESSs' state-of-charge. The complementary constraint $p_{i,t}^{SC} p_{i,t}^{SD} = 0$ preventing simultaneous charging and discharging is omitted according to Proposition 1 in [28], in the sense that the minimized fuel cost or load shedding values will not be affected. The DC power flow model is used in (7i), where $p_{ij,t}^L$ is the active power flow from node i to node j in period t , X_{ij}^L and S_{ij}^L are the reactance and capacity of the line, respectively, and $\theta_{i,t}^B$ denotes the voltage angle. The load demand, load shedding, and the power curtailment at bus i in period t are denoted by $\zeta_{i,t}^D$, $p_{i,t}^D$, and $p_{i,t}^C$, respectively. Their bounds are in (7j). Constraint (7k) is the nodal power balance equation, in which $\zeta_{i,t}^W$ is the wind power generation at bus i in period t .

3.1.2. Operation Problem in Normal Conditions

In normal conditions, the goal is to minimize the total fuel cost of traditional generators.

$$g^N(x, \zeta) := \min_{f^G, p^G, p^{SC}, p^{SD}, e^S, p^L, \theta^B, p^C} \sum_{t \in S^T} \sum_{i \in S^B} f_{i,t}^G \quad (8a)$$

$$\text{s.t. } f_{i,t}^G \geq b_{i,k}^{(1)} p_{i,t}^G \Delta_t + b_{i,k}^{(2)}, \forall k \in \mathcal{K}^b, i \in S^B, t \in S^T \quad (8b)$$

$$p_{i,t}^D = 0, \forall i \in S^B, t \in S^T, (7b) - (7k). \quad (8c)$$

The objective (8a) minimizes the total fuel cost. The fuel cost model in (7a) can be equivalently transformed into inequalities in (8b) thanks to the minimization operation in the objective. The remaining constraints in the power system model are included and the load shedding is forced to be zero in (8c) since no load shedding is allowed in normal conditions. Let $x := (x_i^W, x_i^{SP}, x_i^{SE}; i \in S^B)$ denote the capacity variable and $\zeta := (\zeta_{i,t}^W, \zeta_{i,t}^D; i \in S^B, t \in S^T)$ be the uncertainty realization. When (x, ζ) changes, the optimal objective value (8a) changes accordingly, which is denoted by $g^N(x, \zeta)$.

3.1.3. Operation Problem in Extreme Conditions

In extreme conditions, the goal is to minimize the total load shedding.

$$g^E(x, \zeta) := \min_{p^D, p^G, p^{SC}, p^{SD}, e^S, p^L, \theta^B, p^C} \sum_{t \in S^T} \sum_{i \in S^B} p_{i,t}^D \Delta_t \quad (9a)$$

$$\text{s.t. } (7b) - (7k). \quad (9b)$$

The total load shedding in (9a) is minimized subject to the power system constraints in (9b). Fuel cost is not considered since it is not a major concern in extreme conditions. Similarly, the optimal objective value is a function of x and ζ denoted by $g^E(x, \zeta)$, showing the total load shedding under given (x, ζ) .

3.2. Decision-Dependent Ambiguity Sets

We use ambiguity sets to model uncertainties, formed by a set of distributions around the empirical distribution with distances measured by Wasserstein metric.

3.2.1. Empirical Distributions

Suppose we have some empirical data $(\hat{\zeta}_{i,t,n}^W, \hat{\zeta}_{i,t,n}^D; i \in S^B, t \in S^T), n \in S^E$ of wind and load demand in extreme conditions, where S^E is the index set of extreme scenarios. Then the available wind power is

$$\hat{\zeta}_{i,t,n}^W(x_i^W) = \min \left\{ \min_{k \in \mathcal{K}^a} \{a_{i,k}^{(1)} x_i^W + a_{i,k}^{(2)} \hat{\zeta}_{i,t,n}^W + a_{i,k}^{(3)}\}, \hat{\zeta}_{i,t,n}^W x_i^W \right\}, \quad (10)$$

where $\min_{k \in \mathcal{K}^a} \{a_{i,k}^{(1)} x_i^W + a_{i,k}^{(2)} \hat{\xi}_{i,t,n}^W + a_{i,k}^{(3)}\}$ is the linearized approximation obtained by Algorithm 1; $\hat{\xi}_{i,t,n}^W x_i^W$ is a theoretical upper bound for the available wind power without considering the wake effect and the cut-out wind speed, which can be seen in (4) and (5). The notation $\hat{\xi}_{i,t,n}^W(x_i^W)$ is to emphasize that the available wind power is decision-dependent. Thus, the data of scenario $n \in S^E$ are $\hat{\zeta}_n(x) := (\hat{\zeta}_{i,t,n}^W(x_i^W), \hat{\zeta}_{i,t,n}^D; i \in S^B, t \in S^T)$. Based on the data, the empirical probability distribution $\mathbb{P}_0^E(x)$ in extreme conditions is

$$\mathbb{P}_0^E(x) := \frac{1}{|S^E|} \sum_{n \in S^E} \delta_{\hat{\zeta}_n(x)} = \frac{1}{|S^E|} \sum_{n \in S^E} \left(\bigotimes_{i \in S^B} \delta_{\hat{\zeta}_{i,t,n}^W(x_i^W)} \right) \otimes \delta_{\hat{\zeta}_n^D},$$

where $|S^E|$ is the number of scenarios in S^E , δ denotes the Dirac distribution with unit mass at the subscript point, and \otimes represents the product operation of distributions. Therefore, probability $1/|S^E|$ is assigned to each available wind power sample $\hat{\zeta}_n(x)$ under the empirical distribution $\mathbb{P}_0^E(x)$. Denote the index set of normal scenarios by S^N , then similarly the corresponding empirical distribution $\mathbb{P}_0^N(x)$ can be defined.

3.2.2. Range of Uncertain Variables

For the wind farm at bus i , the range $\Xi_i^{WE}(x_i^W)$ of the wind power output ζ_i^W in extreme conditions is built by

$$\Xi_i^{WE}(x_i^W) := \left\{ \zeta_i^W \left| \begin{array}{l} \zeta_{i,t}^W \leq a_{i,k}^{(1)} x_i^W + a_{i,k}^{(2)} \bar{\xi}_i^W + a_{i,k}^{(3)}, \forall k \in \mathcal{K}^a \\ 0 \leq \zeta_{i,t}^W \leq x_i^W \end{array} \right. \right\}.$$

The wind power $\zeta_{i,t}^W$ cannot exceed the bounds obtained in Algorithm 1 as well as the capacity x_i^W . Again we denote the wind power range by $\Xi_i^{WE}(x_i^W)$ to emphasize the decision-dependent feature.

The range of load demand in extreme conditions is given by $\Xi^{DE} := \{\zeta^D | 0 \leq \zeta_{i,t}^D \leq \bar{\zeta}_i^D\}$, where $\bar{\zeta}_i^D$ is the maximum possible load demand at bus i .

For normal conditions, the range is defined as the convex hull of the corresponding scenarios. Then the range of wind power ζ_i^W in normal conditions is

$$\Xi_i^{WN}(x_i^W) := \left\{ \zeta_i^W = \sum_{n \in S^N} \lambda_n \hat{\zeta}_{i,t,n}^W(x_i^W) \left| \lambda_n \geq 0, \sum_{n \in S^N} \lambda_n = 1 \right. \right\},$$

where $\lambda_n, n \in S^N$ are the coefficients of convex combination; all the convex combinations of $\hat{\zeta}_{i,t,n}^W(x_i^W), n \in S^N$ are contained in $\Xi_i^{WN}(x_i^W)$, which is also decision-dependent. The range Ξ^{DN} of load demand in normal conditions has a similar form. The range of uncertain variables in extreme conditions is larger than that in normal conditions to include the possible extreme scenarios, i.e., $\Xi_i^{WN}(x_i^W) \subset \Xi_i^{WE}(x_i^W)$ and $\Xi^{DN} \subset \Xi^{DE}$.

3.2.3. Wasserstein Metric and Ambiguity Set

Wasserstein metric is a way to measure the distance between two distributions [29]. For distributions \mathbb{P}_1 and \mathbb{P}_2 defined on Ξ , the 1-norm Wasserstein metric between them is

$$d^W(\mathbb{P}_1, \mathbb{P}_2) := \inf_{\Pi} \int_{\Xi^2} \|\zeta_1 - \zeta_2\|_1 \Pi(d\zeta_1, d\zeta_2) \quad (11)$$

Π is a joint distribution with marginals \mathbb{P}_1 and \mathbb{P}_2 ,

where $\|\cdot\|_1$ is the 1-norm. It can be regarded as the minimum cost of transporting the mass distribution \mathbb{P}_1 to \mathbb{P}_2 , in which the transport way is represented by the joint distribution Π .

Inspired by the definition of Wasserstein metric, we propose the following ambiguity set $\mathcal{B}^E(\varepsilon^E, x)$ for uncertain variable ζ in extreme conditions.

$$\begin{aligned}
\mathcal{B}^E(\varepsilon^E, x) &:= \left\{ \frac{1}{|S^E|} \sum_{n \in S^E} \left(\bigotimes_{i \in S^B} \mathbb{P}_{i,n}^W \right) \otimes \mathbb{P}_n^D \right\} \\
\mathbb{P}_{i,n}^W &\in \mathcal{M}(\Xi_i^{WE}(x_i^W)), \Pi_i^W = \frac{1}{|S^E|} \sum_{n \in S^E} \mathbb{P}_{i,n}^W \otimes \delta_{\zeta_{i,n}^W(x_i^W)} \\
\int_{(\Xi_i^{WE}(x_i^W))^2} \|\zeta_i^W - \tilde{\zeta}_i^W\|_1 \Pi_i^W(d\zeta_i^W, d\tilde{\zeta}_i^W) &\leq \varepsilon_i^{WE} x_i^W, \forall i \in S^B \\
\mathbb{P}_n^D &\in \mathcal{M}(\Xi^{DE}), \Pi^D = \frac{1}{|S^E|} \sum_{n \in S^E} \mathbb{P}_n^D \otimes \delta_{\zeta_n^D} \\
\int_{(\Xi^{DE})^2} \|\zeta^D - \tilde{\zeta}^D\|_1 \Pi^D(d\zeta^D, d\tilde{\zeta}^D) &\leq \varepsilon^{DE} \}.
\end{aligned} \tag{12}$$

The distributions in $\mathcal{B}^E(\varepsilon^E, x)$ are the average of the product distributions of $\mathbb{P}_{i,n}^W$ and \mathbb{P}_n^D . $\mathcal{M}(\cdot)$ denotes the set of all the distributions supported on the range in the bracket. Π_i^W is a joint distribution with marginals $\frac{1}{|S^E|} \sum_{n \in S^E} \mathbb{P}_{i,n}^W$ and empirical distribution $\frac{1}{|S^E|} \sum_{n \in S^E} \delta_{\zeta_{i,n}^W(x_i^W)}$. The Wasserstein metric between them is no larger than $\varepsilon_i^{WE} x_i^W$, where ε_i^{WE} is a parameter controlling the size of the ambiguity set. Since larger capacity leads to larger fluctuation of wind power, we use the product $\varepsilon_i^{WE} x_i^W$ as the bound. The constraints of load demand distribution \mathbb{P}_n^D have a similar bound ε^{DE} . Let $\varepsilon^E := (\varepsilon_i^{WE}, \varepsilon^{DE}; i \in S^E)$, then the ambiguity set contains $\mathbb{P}_0^E(x)$ for all non-negative ε^E and it becomes a singleton when $\varepsilon^E = 0$, the zero vector.

The ambiguity set $\mathcal{B}^N(\varepsilon^N, x)$ in normal conditions can be defined similarly by replacing S^E , Ξ_i^{WE} , Ξ^{DE} , ε_i^{WE} , and ε^{DE} by S^N , Ξ_i^{WN} , Ξ^{DN} , ε_i^{WN} , and ε^{DN} , respectively. Both the ambiguity sets are decision-dependent.

There are theoretical results about the convergence rate of empirical distributions under Wasserstein metric [30], which guide the proper selection of the Wasserstein metric bounds ε^E and ε^N . Roughly speaking, the bound should be proportional to $\sup_{\zeta_1, \zeta_2 \in \Xi} \|\zeta_1 - \zeta_2\|_1$ and $1/N^{1/M}$, where N is the number of data and M is the dimension.

Some literature on Wasserstein-metric-based DRO uses the ambiguity sets that only contain the discrete distributions supported on the sample data sets [31], which are not suitable for wind power and load demand uncertainties because they can change continuously. Therefore, the Wasserstein-metric-based ambiguity sets constructed in this paper contain general distributions including both continuous and discrete ones.

3.3. Sizing Model

Suppose \bar{x}_i^W , \bar{x}_i^{SP} , and \bar{x}_i^{SE} are the upper bounds of x_i^W , x_i^{SP} , and x_i^{SE} , respectively. Then the feasible set of capacity variable x is as follows.

$$\mathcal{X} := \left\{ x \left| \begin{array}{l} 0 \leq x_i^W \leq \bar{x}_i^W, 0 \leq x_i^{SP} \leq \bar{x}_i^{SP}, 0 \leq x_i^{SE} \leq \bar{x}_i^{SE}, \forall i \in S^B \\ g^N(x, \hat{\zeta}_n) < +\infty, \forall n \in S^N \end{array} \right. \right\},$$

where $g^N(x, \hat{\zeta}_n) < +\infty, \forall n \in S^N$ means that the operation problem (8) is feasible for all normal scenarios; in other words, load shedding will not arise in normal conditions. Since $g^N(x, \zeta)$ is the optimal value of a linear program (LP), it is a convex function on its domain [32].

The bi-objective sizing model is established below.

$$\min_{x \in \mathcal{X}} \left\{ \sum_{i \in S^B} (C_i^W x_i^W + C^{SP} x_i^{SP} + C^{SE} x_i^{SE}), I^F \right\} \tag{13a}$$

$$\text{s.t.} \quad \sup_{\mathbb{P} \in \mathcal{B}^E(\varepsilon^E, x)} \mathbb{E}_{\mathbb{P}}[g^E(x, \zeta)] \leq \bar{g}^E \quad (13b)$$

$$I^F = \sup_{\mathbb{P} \in \mathcal{B}^N(\varepsilon^N, x)} \mathbb{E}_{\mathbb{P}}[g^N(x, \zeta)], \quad (13c)$$

where in (13a) the first objective is to minimize the total investment cost, and the second objective function defined in (13c) represents the worst-case fuel cost expectation when the distribution \mathbb{P} varies within the ambiguity set $\mathcal{B}^N(\varepsilon^N, x)$ for normal conditions. Constraint (13b) stipulates an upper bound \bar{g}^E for the worst-case load shedding expectation in extreme conditions. The worst-case distributions in normal and extreme conditions are different. In (13), the wind farm capacities are approximated by continuous variables. If the obtained capacity is not divisible by the capacity of a single WT, we round the obtained capacity to the nearest integer multiples of the WT capacity to ensure the number of WTs is an integer. For large-scale wind farms, this simplification would not significantly affect the optimality, as will be examined in Section 5.

The sizing model (13) is hard to solve due to three reasons: 1) There are distributionally robust expectations in the model. 2) The ambiguity sets are decision-dependent. 3) The functions $g^E(x, \zeta)$ and $g^N(x, \zeta)$ are defined as the optimal values of LP problems. To overcome these difficulties, we develop a solution method in the next section.

4. Solution Method

We first transform the DRO sizing model (13) into a SP problem, and then propose an iterative algorithm to solve it.

4.1. Approximate Stochastic Programming Problem

First, we use Lipschitz constants to transform the distributionally robust expectations into the expectations with respect to the empirical distributions plus compensation terms, as in the following theorem.

Theorem 1. For any $x \in \mathcal{X}$ and $\varepsilon^E \geq 0$,

$$\begin{aligned} & \sup_{\mathbb{P} \in \mathcal{B}^E(\varepsilon^E, x)} \mathbb{E}_{\mathbb{P}}[g^E(x, \zeta)] \\ & \leq \sum_{i \in S^B} \varepsilon_i^{WE} x_i^W L_i^{WE}(x) + \varepsilon^{DE} L^{DE}(x) + \mathbb{E}_{\mathbb{P}_0^E(x)}[g^E(x, \zeta)], \end{aligned} \quad (14)$$

where $L_i^{WE}(x)$ is the minimum Lipschitz constant of $g^E(x, \zeta)$ regarded as a function of ζ_i^W , and $L^{DE}(x)$ is the minimum Lipschitz constant of $g^E(x, \zeta)$ regarded as a function of ζ^D .¹

The proof of Theorem 1 can be found in Appendix A. The distributionally robust expectation in normal conditions has a similar property with minimum Lipschitz constants $L_i^{WN}(x)$ and $L^{DN}(x)$.

By the sample average approximation (SAA) technique, $\mathbb{E}_{\mathbb{P}_0^E(x)}[g^E(x, \zeta)] = \sum_{n \in S^E} g^E(x, \hat{\zeta}_n(x)) / |S^E|$. Thus, the following SP problem is an approximation of the sizing model (13).

$$\min \left\{ \sum_{i \in S^B} (C_i^W x_i^W + C^{SP} x_i^{SP} + C^{SE} x_i^{SE}), I^F \right\} \quad (15a)$$

¹For example,

$$L_i^{WE}(x) := \inf \left\{ L \left| \begin{array}{l} |g^E(x, \zeta) - g^E(x, \tilde{\zeta})| \leq L \|\zeta_i^W - \tilde{\zeta}_i^W\|_1 \\ \forall \zeta_i^W, \tilde{\zeta}_i^W \in \Xi_i^{WE}(x_i^W), \text{ s.t. } \zeta^D = \tilde{\zeta}^D \in \Xi^{DE} \\ \zeta_j^W = \tilde{\zeta}_j^W \in \Xi_j^{WE}(x_j^W), \forall j \neq i \end{array} \right. \right\}.$$

$$\text{s.t. } 0 \leq x_i^W \leq \bar{x}_i^W, 0 \leq x_i^{SP} \leq \bar{x}_i^{SP}, 0 \leq x_i^{SE} \leq \bar{x}_i^{SE}, \forall i \in S^B \quad (15b)$$

$$\sum_{i \in S^B} \varepsilon_i^{WE} x_i^W L_i^{WE}(x) + \varepsilon^{DE} L^{DE}(x) + \frac{1}{|S^E|} \sum_{n \in S^E} g_n^E \leq \bar{g}^E \quad (15c)$$

$$g_n^E \geq \sum_{t \in S^T} \sum_{i \in S^B} p_{i,t,n}^D \Delta_t, (9b), \forall n \in S^E \quad (15d)$$

$$I^F = \sum_{i \in S^B} \varepsilon_i^{WN} x_i^W L_i^{WN}(x) + \varepsilon^{DN} L^{DN}(x) + \frac{1}{|S^N|} \sum_{n \in S^N} g_n^N \quad (15e)$$

$$g_n^N \geq \sum_{t \in S^T} \sum_{i \in S^B} f_{i,t,n}^G, (8b), (8c), \forall n \in S^N \quad (15f)$$

$$\zeta_{i,t,n}^W \leq a_{i,k}^{(1)} x_i^W + a_{i,k}^{(2)} \hat{\zeta}_{i,t,n}^W + a_{i,k}^{(3)}, \forall k \in \mathcal{K}^a, n \in S^E \cup S^N \quad (15g)$$

$$0 \leq \zeta_{i,t,n}^W \leq \hat{\zeta}_{i,t,n}^W x_i^W, \forall i \in S^B, n \in S^E \cup S^N, \quad (15h)$$

where (15b) and (15f) contain the requirement $x \in \mathcal{X}$; g_n^E and g_n^N are auxiliary variables representing $g^E(x, \zeta_n(x))$ and $g^N(x, \zeta_n(x))$, respectively. As will be examined in Section 5, the approximate problem is not over-conservative with suitable parameters ε^E and ε^N .

4.2. Solution Algorithm

To solve the SP problem (15), we still need to address two issues: 1) what are the minimum Lipschitz constants $L_i^{WE}(x)$, $L^{DE}(x)$, $L_i^{WN}(x)$, and $L^{DN}(x)$; 2) how to solve the bi-objective optimization.

For the first issue, though the minimum Lipschitz constants are hard to calculate accurately, it is easy for us to obtain their upper bounds based on the fact that functions $g^E(x, \zeta)$ and $g^N(x, \zeta)$ are defined by LPs whose dual variables can reflect their changing rates in ζ . Denote the upper bounds by $\tilde{L}_i^{WE}(x)$, $\tilde{L}^{DE}(x)$, $\tilde{L}_i^{WN}(x)$, and $\tilde{L}^{DN}(x)$, respectively. The detailed procedure for getting the upper bounds is presented in Appendix B. According to the procedure, we can find that calculating $\tilde{L}_i^{WE}(x)$ and $\tilde{L}^{DE}(x)$ involves solving a KKT condition embedded optimization while calculating $\tilde{L}_i^{WN}(x)$ and $\tilde{L}^{DN}(x)$ only requires solving some LP problems. To accelerate the computation, we use uniform upper bounds for $L_i^{WE}(x)$ and $L^{DE}(x)$, i.e., $\tilde{L}_i^{WE} \geq L_i^{WE}(x)$, $\tilde{L}^{DE} \geq L^{DE}(x)$, $\forall x \in \mathcal{X}$; and x -dependent upper bounds for $\tilde{L}_i^{WN}(x)$ and $\tilde{L}^{DN}(x)$, i.e., $\tilde{L}_i^{WN}(x) \geq L_i^{WN}(x)$ and $\tilde{L}^{DN}(x) \geq L^{DN}(x)$.

For the second issue, we adopt the ε -constraint method [33] to handle the two objectives. Particularly, the investment cost objective is replaced with a budget constraint, and the new model only minimizes the fuel cost expectation as follows.

$$\begin{aligned} & \min I^F \\ & \text{s.t. (15b) – (15h)} \\ & \sum_{i \in S^B} (C_i^W x_i^W + C^{SP} x_i^{SP} + C^{SE} x_i^{SE}) \leq \bar{C}, \end{aligned} \quad (16)$$

where \bar{C} is the budget. With a varying budget, the Pareto frontier of the bi-objective sizing model can be obtained, which is the advantage of the ε -constraint method compared with summing the two objective functions together. The uniform upper bounds \tilde{L}_i^{WE} and \tilde{L}^{DE} are calculated in advance and used in the solution process of (16), which is shown in Algorithm 2. The algorithm finds an approximate solution in an iterative way: in each iteration k , use the $\tilde{L}_i^{WN}(x_k)$ and $\tilde{L}^{DN}(x_k)$ in the current iteration to approximate the upper bounds of minimum Lipschitz constants in the next iteration by letting $L_i^{WN} \leftarrow \tilde{L}_i^{WN}(x_k)$, $\forall i \in S^B$, $L^{DN} \leftarrow \tilde{L}^{DN}(x_k)$.

Algorithm 2: Iterative Algorithm for Problem (16)

Input: Parameters of problem (13), budget \bar{C} , error tolerance $\varepsilon > 0$, and uniform upper bounds \tilde{L}_i^{WE} and \tilde{L}^{DE} .

Output: Solution x_k and the corresponding distributionally robust expectation of fuel cost I^F .

- 1: Initiation: Let $L_i^{WN} \leftarrow 0, \forall i \in S^B, L^{DN} \leftarrow 0, k \leftarrow 0$, and $x_k \leftarrow 0$.
- 2: Solve the LP problem

$$\begin{aligned} \min \quad & \sum_{i \in S^B} \varepsilon_i^{WN} x_i^W L_i^{WN} + \varepsilon^{DN} L^{DN} + \frac{1}{|S^N|} \sum_{n \in S^N} g_n^N \\ \text{s.t.} \quad & \sum_{i \in S^B} (C_i^W x_i^W + C^{SP} x_i^{SP} + C^{SE} x_i^{SE}) \leq \bar{C} \\ & \sum_{i \in S^B} \varepsilon_i^{WE} x_i^W \tilde{L}_i^{WE} + \varepsilon^{DE} \tilde{L}^{DE} + \frac{1}{|S^E|} \sum_{n \in S^E} g_n^E \leq \bar{g}^E \end{aligned}$$

(15b), (15d), (15f) – (15h).

If it is infeasible, terminate. Otherwise, update $k \leftarrow k + 1$; let x_k be the optimal solution and I^F be the optimal value.

- 3: If $k > 0$ and $\|x_k - x_{k-1}\| \leq \varepsilon$, output results and terminate. Otherwise, calculate and let $L_i^{WN} \leftarrow \tilde{L}_i^{WN}(x_k), \forall i \in S^B, L^{DN} \leftarrow \tilde{L}^{DN}(x_k)$, then go to Step 2.
-

5. Case Studies

This section first uses a modified IEEE 30-bus system to test the proposed method. The influence of the wake effect on the sizing results is examined and the proposed method is compared with the traditional SP and RO methods. Sensitivity analysis is also conducted. Moreover, the scalability of the proposed method is verified via a modified IEEE 118-bus system. All experiments are performed on a laptop equipped with Intel i7-12700H processor and 16 GM RAM. The LPs and mixed-integer linear programs (MILPs) are solved by GUROBI 9.5 in MATLAB.

5.1. Benchmark

The benchmark case study is based on a modified IEEE 30-bus system, whose data can be found in [34] and some parameters are listed in Table 1. There are candidate wind farms at buses 13 and 27, where the WT parameters are from [35]. The candidate wind farms are built on square areas with 25 and 20 rows, respectively. The wind speed data are generated based on the weather data in Qinghai province, China [36]. There are candidate ESSs at buses 13, 23, and 27. They all have capacity bounds $\bar{x}^{SP} = 1$ GW and $\bar{x}^{SE} = 5$ GWh. The load demand data are generated by normal distributions with bounds. We generate 365 groups of data in total. By analyzing the load demand and wind conditions, we select 89 groups from them to represent extreme conditions, and another 272 groups are for normal conditions. In the benchmark case, $|S^E| = 24$ and $|S^N| = 72$ groups of data are used for sizing. In the out-of-sample tests, 65 and 200 groups of data are used for validation, representing the distributions of extreme conditions and normal conditions, respectively. The parameters ε^E and ε^N controlling the size of the ambiguity sets are set as

$$\begin{aligned} \varepsilon_i^{WE} &= \varepsilon_0 / |S^E|^{1/T}, i = 13, 27, \varepsilon^{DE} = 20\varepsilon_0 / |S^E|^{1/(20T)}, \\ \varepsilon_i^{WN} &= \varepsilon_0 / |S^N|^{1/T}, i = 13, 27, \varepsilon^{DN} = 20\varepsilon_0 / |S^N|^{1/(20T)}, \end{aligned}$$

where 20 is the number of buses with load, and $\varepsilon_0 = 0.05$ is an auxiliary scalar parameter to control ε^E and ε^N .

Table 1: Parameters

Parameter	Value	Parameter	Value
T	24	Δ_t	1 h
η^{SC}	0.95	η^{SD}	0.95
ω^S	0.10	$\bar{\omega}^S$	0.90
C^{SP}	1.0×10^6 CNY/MW	C^{SE}	1.2×10^6 CNY/MWh
C^W	5.5×10^6 CNY/MW	\bar{g}^E	220 MWh

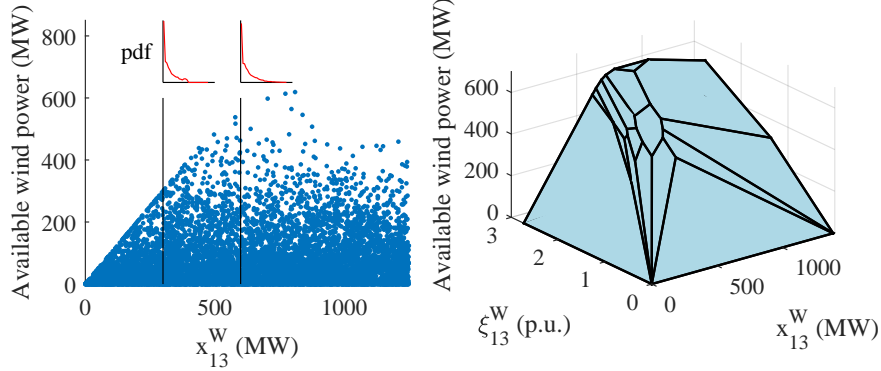


Figure 3: Available wind power samples and linearized available wind power function at bus 13.

To visualize the endogenous uncertainty, we draw the available wind power sample points in Figure 3 (left), where the points with the same horizontal coordinate reflect the distribution and probability density function (pdf) of the available wind power under a specific wind power capacity. It is clear that the distributions change as the capacity varies. The linearized available wind power function proposed in Section 2 is shown in Figure 3 (right). The total computation time is within 1 s. The errors between the available wind power model (10) and the simulation value are about 5% on average, mainly from the convex hull approximation.

The sizing results with different investment budgets are shown in Figure 4. The minimum investment is 2.83×10^8 CNY to equip ESSs and ensure the reliable supply of load demand. When the investment budget increases, the capacities of the wind power generation become larger because renewable power can help reduce fuel costs. The wind power generation capacity accounts for about 30% of the total generation capacity when the investment budget is 32×10^8 CNY. The total capacity of ESSs does not change much when wind power penetration is relatively low, but starts to grow with more wind power generation due to the flexibility requirement in the power system. We compare the results before and after the obtained capacity is rounded to integer multiples of the single WT capacity, and the error is below 0.5%. Therefore, we can optimize with continuous capacity variables and then round the results without perceptible loss of optimality. Moreover, all fuel costs and load shedding in this section have been verified to remain the same after adding the charging and discharging complementarity constraints to the power system model (7).

5.2. Comparison With Traditional Methods

In order to show the impact of the wake effect and the advantage of the DRO technique, we compare the proposed method with traditional methods:

- DRO: The proposed method.
- SP1: Traditional SP method that does not consider the wake effect. In this method, the empirical distributions are regarded as the real distributions, i.e., $\sup_{\mathbb{P} \in \mathcal{B}^E(\varepsilon^E, x)} \mathbb{E}_{\mathbb{P}}[g^E(x, \zeta)]$ and $\sup_{\mathbb{P} \in \mathcal{B}^N(\varepsilon^N, x)} \mathbb{E}_{\mathbb{P}}[g^N(x, \zeta)]$

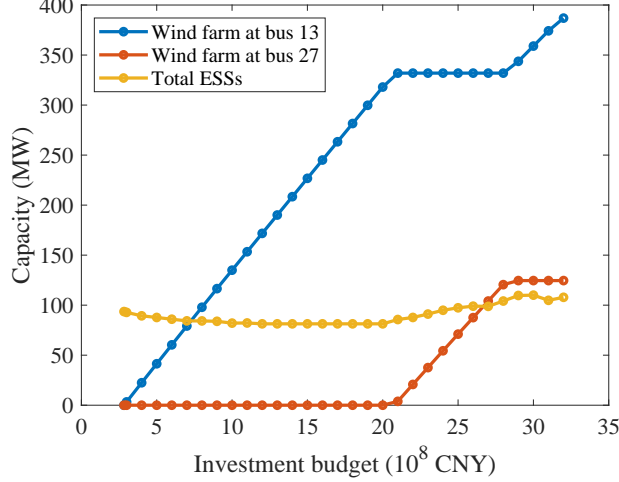


Figure 4: Sizing results of the modified IEEE 30-bus system.

are replaced by $\mathbb{E}_{\mathbb{P}_0^E(x)}[g^E(x, \zeta)]$ and $\mathbb{E}_{\mathbb{P}_0^N(x)}[g^N(x, \zeta)]$, respectively. The wake effect is not considered, so the available wind power in (10) becomes $\hat{\zeta}_{i,t,n}^W(x_i^W) = \hat{\xi}_{i,t,n}^W x_i^W$. The sizing model can be equivalently transformed into an LP following a similar solution method to that described in Section 4.

- SP2: Traditional SP method considering the wake effect. This method is similar to SP1 except that the available wind power is still computed according to (10).
- RO: RO method considering the wake effect. This method optimizes over the worst cases in $\tilde{\Xi}^E(x) := \{\hat{\zeta}_n(x) | n \in S^E\}$ and $\tilde{\Xi}^N(x) := \{\hat{\zeta}_n(x) | n \in S^N\}$. The sizing model is

$$\begin{aligned} \min_{x \in \mathcal{X}} \left\{ \sum_{i \in S^B} (C_i^W x_i^W + C^{SP} x_i^{SP} + C^{SE} x_i^{SE}), \sup_{n \in S^N} g^N(x, \hat{\zeta}_n(x)) \right\} \\ \text{s.t. } \sup_{n \in S^E} g^E(x, \hat{\zeta}_n(x)) \leq \bar{g}^E. \end{aligned}$$

Their Pareto frontiers are depicted in Figure 5. First, we compare the impact of wake effect. The Pareto frontiers of SP1 and SP2 almost coincide when the investment budget is below 17×10^8 CNY because the capacities of wind power generation are relatively small and the wake effect is not obvious, as shown in Figure 3. As the investment budget gets higher, the difference between the Pareto frontiers of SP1 and SP2 enlarges. The estimated fuel cost of SP1 becomes remarkably lower than that of SP2, showing that neglecting wake effect results in an over-optimistic estimate of fuel cost. Therefore, it is necessary to consider the wake effect in future power systems that will have large-scale wind power.

Then, we compare SP2, RO, and DRO. They all take into account the wake effect but use different optimization techniques to deal with uncertainties. The Pareto frontier of DRO is above SP2 and below RO. The minimum feasible investment budget of DRO is also in-between those of SP2 and RO. This shows the results of DRO are much less conservative than RO though a little bit more costly than SP2.

In order to compare the different methods in more detail, we list the sizing results under the investment budget 30×10^8 CNY in Table 2, where the estimated g^E and g^N are obtained from the corresponding optimization methods, while the tested g^E and g^N are average values given by the out-of-sample tests. In terms of the estimated fuel cost g^N , we have $SP1 < SP2 < DRO < RO$, from the most optimistic to the most conservative methods. Following this order, the total capacity of ESSs increases, and that of wind power generation decreases. This is because low-cost wind power generation brings uncertainties to the system

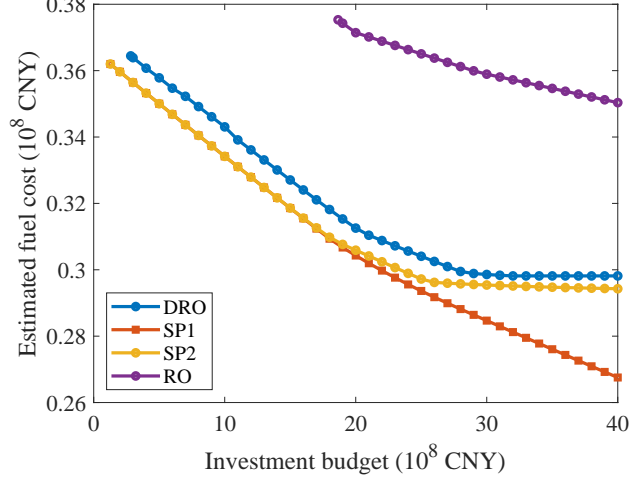


Figure 5: Comparison of Pareto frontiers.

Table 2: Comparison of sizing results

Method	DRO	SP1	SP2	RO
(x_{13}^W, x_{27}^W) (MW)	(359, 125)	(497, 41)	(383, 125)	(99, 125)
$(x_{13}^{SP}, x_{23}^{SP}, x_{27}^{SP})$ (MW)	(55, 0, 55)	(0, 4, 15)	(40, 0, 10)	(196, 145, 266)
$(x_{13}^{SE}, x_{23}^{SE}, x_{27}^{SE})$ (MWh)	(119, 0, 73)	(0, 5, 19)	(127, 0, 13)	(258, 191, 521)
Estimated g^E (MWh)	220	199	129	0
Tested g^E (MWh)	73	223	133	1
Estimated g^N (10^8 CNY)	0.2986	0.2847	0.2954	0.3589
Tested g^N (10^8 CNY)	0.2959	0.3045	0.2957	0.3326

while the ESSs can provide flexibility. The estimated load shedding g^E is within the upper bound 220 MWh under all the methods, but the tested g^E of SP1 exceeds the bound. The tested g^E of DRO is 73 MWh, which is higher than that of RO but much lower than those of SP1 and SP2. The tested g^N of SP1 and SP2 are higher than the estimated value because the distribution represented by the test data is different from the empirical distribution but the SP-based methods neglect the possible inexactness of empirical distribution. On the contrary, the tested g^N under DRO is lower than the estimated one because this method already considers the inexactness of empirical distribution and the test distribution is better than the worst-case distribution. For the tested g^N , we have $SP2 \approx DRO < SP1 < RO$. Considering that the DRO method performs better in load shedding than SP2 and has a lower cost than RO, DRO stands out among others in that it achieves a good balance between optimality and robustness.

5.3. Sensitivity Analysis

In the sensitivity analysis, we investigate the impacts of the scalar parameter ϵ_0 of ambiguity set size, maximum acceptable load shedding expectation \bar{g}^E in extreme conditions, and the unit cost of ESS. In this subsection, we set an upper bound 0.31×10^8 CNY for the estimated g^N and minimize the investment cost. The results under different ϵ_0 are shown in Table 3. Larger ϵ_0 leads to larger ambiguity sets and more conservative results, which can be seen from the increasing investment and decreasing tested g^E and g^N . Note that the tested g^N exceeds the upper bound when $\epsilon_0 = 0.01$ and 0.02 , which indicates that the ambiguity sets are not large enough to include the distribution represented by the test data. Proper parameters should be selected to establish an ambiguity set with a suitable size so that the sizing results are robust but not over-conservative.

Table 3: Results under different ϵ_0

ϵ_0	0.01	0.02	0.05	0.08
(x_{13}^W, x_{27}^W) (MW)	(321, 0)	(326, 0)	(332, 9)	(332, 26)
$(x_{13}^{SP}, x_{23}^{SP}, x_{27}^{SP})$ (MW)	(0, 0, 31)	(0, 0, 44)	(13, 0, 74)	(5, 0, 161)
$(x_{13}^{SE}, x_{23}^{SE}, x_{27}^{SE})$ (MWh)	(0, 0, 41)	(0, 0, 60)	(17, 0, 124)	(6, 0, 280)
Investment (10^8 CNY)	18.45	19.09	21.26	24.78
Tested g^E (MWh)	208	184	110	37
Tested g^N (10^8 CNY)	0.3110	0.3104	0.3087	0.3068

Table 4: Results under different \bar{g}^E

\bar{g}^E (MWh)	150	220	290	360
(x_{13}^W, x_{27}^W) (MW)	(332, 8)	(332, 9)	(332, 9)	(332, 9)
$(x_{13}^{SP}, x_{23}^{SP}, x_{27}^{SP})$ (MW)	(7, 0, 147)	(13, 0, 74)	(7, 0, 38)	(0, 4, 15)
$(x_{13}^{SE}, x_{23}^{SE}, x_{27}^{SE})$ (MWh)	(9, 0, 257)	(17, 0, 124)	(9, 0, 49)	(0, 5, 20)
Investment (10^8 CNY)	23.44	21.26	19.88	19.24
Tested g^E (MWh)	42	110	183	228
Tested g^N (10^8 CNY)	0.3087	0.3087	0.3087	0.3085

Table 5: Results under different κ

κ	0.6	0.8	1.0	1.2
(x_{13}^W, x_{27}^W) (MW)	(332, 8)	(332, 8)	(332, 9)	(332, 9)
$(x_{13}^{SP}, x_{23}^{SP}, x_{27}^{SP})$ (MW)	(14, 0, 73)	(13, 0, 74)	(13, 0, 74)	(12, 0, 75)
$(x_{13}^{SE}, x_{23}^{SE}, x_{27}^{SE})$ (MWh)	(18, 0, 122)	(17, 0, 123)	(17, 0, 124)	(16, 0, 125)
Investment (10^8 CNY)	20.24	20.75	21.26	21.77

Table 6: Computation time of Algorithm 2 under different settings

Number of scenarios	48	96	144	192
30-bus	31 s	53 s	145 s	184 s
118-bus	75 s	210 s	374 s	512 s

Table 4 shows the results under different \bar{g}^E . The larger the \bar{g}^E is, the smaller the investment cost becomes. The capacities of ESSs change much while that of wind power generation are almost the same. The reason is that larger ESSs help to enhance reliability. Note that the tested g^E is always lower than \bar{g}^E and the tested g^N is within the bounds, which shows the proposed method is effective.

We investigate the impact of the ESS unit cost by multiplying C^{SP} and C^{SE} by a constant κ . The results under different κ are listed in Table 5. As κ increases, the investment cost becomes larger, while the capacities of wind power generation and ESSs do not change much, indicating that ESSs and wind power play different roles in the system and they can hardly substitute each other even when the unit cost changes.

5.4. Scalability

To show the scalability of the proposed method, a modified IEEE 118-bus system is tested, where candidate components are 4 wind farms, 2 PV stations, and 3 ESSs. The PV stations are treated in a similar way but without wake effect. The sizing results are shown in Figure 6. ESSs will be invested when the renewable capacity is large. Table 6 shows the computation time of Algorithm 2 under different settings. Overall, the computation efficiency is acceptable for planning purposes.

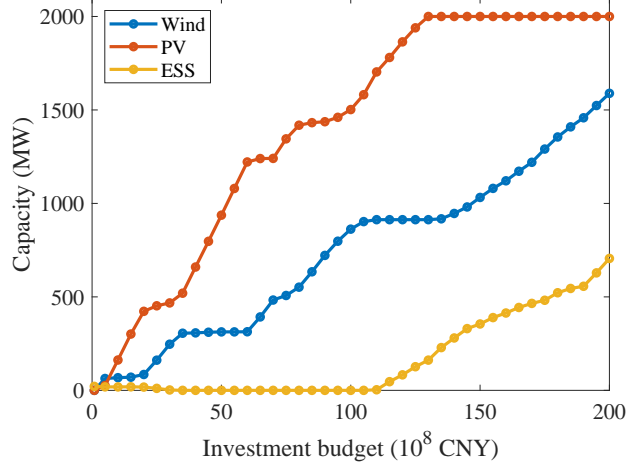


Figure 6: Sizing results of the modified IEEE 118-bus system.

6. Conclusion

This paper studies the sizing problem of wind power generation and energy storage in power systems considering the wake effect, which is cast as a DRO model with DDU. A solution methodology consisting of the SP approximation based on minimum Lipschitz constants, evaluations of the Lipschitz constants, and an iterative algorithm, is developed. Simulations on the modified IEEE 30-bus and 118-bus systems show the effectiveness and scalability of the proposed method, and reveal the following findings: 1) The impact of wake effect becomes more significant when the wind power capacity grows in a limited area. 2) The DRO model outperforms the traditional SP and RO models in terms of balancing optimality and robustness.

Our future work aims at considering the long-term uncertainties from society, economy, and technology.

Acknowledgments

This work was supported by the CUHK Direct Grant for Research [grant number 4055169].

Appendix A. Proof of Theorem 1

We omit function variable x in the proof since it can be regarded as a fixed parameter of the function. We investigate the properties of the function $g^E(\zeta)$ first and then transform the distributionally robust expectation.

Appendix A.1. Load Shedding Function

The definition of $g^E(\zeta)$ in (9) can be written in a compact form as follows.

$$\begin{aligned} \forall \zeta \in \Xi^E, g^E(\zeta) := \min_y C^\top y \\ \text{s.t. } Ay \geq B\zeta + D, \end{aligned} \quad (\text{A.1})$$

where A , B , C , and D are coefficient matrices or vectors; y denotes the operation variables. Since $g^E(\zeta)$ represents the minimum load shedding, it is always nonnegative and no larger than the total load demand. Thus, the LP problem (A.1) has a finite optimal value. Then by the strong duality of LP [32], we have

$$\forall \zeta \in \Xi^E, g^E(\zeta) = \max_{\pi} \pi^\top B\zeta + \pi^\top D$$

$$\text{s.t. } A^\top \pi = C, \pi \geq 0.$$

Because the optimal value can be reached at some vertex if it is finite,

$$\forall \zeta \in \Xi^E, g^E(\zeta) = \max_{\pi \in V(\Pi)} \left\{ \pi^\top B \zeta + \pi^\top D \right\}, \quad (\text{A.2})$$

with polyhedron $\Pi := \{\pi | A^\top \pi = C, \pi \geq 0\}$ and its vertex set $V(\Pi)$. Then $V(\Pi)$ is a finite set and g^E is convex [32] and continuous. For each $\pi \in V(\Pi)$, let

$$\Xi_\pi := \{\zeta \in \Xi^E | g^E(\zeta) = \pi^\top B \zeta + \pi^\top D\},$$

then it is either empty or closed, and $\bigcup_{\pi \in V(\Pi)} \Xi_\pi = \Xi^E$.

Claim 1: For $\pi \in V(\Pi)$, if $\Xi_\pi \neq \emptyset$, then it is convex.

Proof: Suppose $\zeta, \check{\zeta} \in \Xi_\pi$ and $\lambda \in [0, 1]$. Then

$$\pi^\top B(\lambda \zeta + (1-\lambda)\check{\zeta}) + \pi^\top D \quad (\text{A.3})$$

$$= \lambda(\pi^\top B \zeta + \pi^\top D) + (1-\lambda)(\pi^\top B \check{\zeta} + \pi^\top D)$$

$$= \lambda g^E(\zeta) + (1-\lambda)g^E(\check{\zeta})$$

$$\geq g^E(\lambda \zeta + (1-\lambda)\check{\zeta}) \quad (\text{A.4})$$

$$\geq \pi^\top B(\lambda \zeta + (1-\lambda)\check{\zeta}) + \pi^\top D, \quad (\text{A.5})$$

where (A.4) follows from the convexity of g^E and (A.5) is due to (A.2). Since (A.3) and (A.5) are the same, the inequalities are actually equations, so $\lambda \zeta + (1-\lambda)\check{\zeta} \in \Xi_\pi$ and therefore Ξ_π is convex. \square

Let \tilde{V} be a subset of $V(\Pi)$ defined by

$$\tilde{V} := \{\pi \in V(\Pi) | \exists \text{ open set } U \text{ s.t. } U \subset \Xi_\pi\}.$$

In addition, define a new function $\tilde{g} : \mathbb{R}^M \rightarrow \mathbb{R}$ as follows, where M is the dimension of ζ .

$$\tilde{g}(\zeta) := \max_{\pi \in \tilde{V}} \left\{ \pi^\top B \zeta + \pi^\top D \right\}, \forall \zeta \in \mathbb{R}^M. \quad (\text{A.6})$$

We prove that $\tilde{g}(\zeta)$ is an extension of $g^E(\zeta)$.

Claim 2: $\tilde{g}(\zeta) = g^E(\zeta), \forall \zeta \in \Xi^E$.

Proof: Denote the Lebesgue measure by $m(\cdot)$. For any $\pi \in V(\Pi)$, if $m(\Xi_\pi) > 0$, then Ξ_π contains some open set since it is convex. Additionally, $|V(\Pi)| < \infty$, so $m(\bigcup_{\pi \in V(\Pi) \setminus \tilde{V}} \Xi_\pi) = 0$. Thus, $m(\bigcup_{\pi \in \tilde{V}} \Xi_\pi) = m(\bigcup_{\pi \in V(\Pi)} \Xi_\pi) = m(\Xi^E) > 0$ and it is finite since Ξ^E is bounded. Note that Ξ^E is convex, $\tilde{g} = g^E$ on $\bigcup_{\pi \in \tilde{V}} \Xi_\pi$, and they are continuous, so $\tilde{g}(\zeta) = g^E(\zeta), \forall \zeta \in \Xi^E$. \square

Because $\tilde{g}(\zeta)$ is proper, convex, and continuous, according to the property of conjugate function [37], $\tilde{g} = \tilde{g}^{**}$, which is the bi-conjugate function, i.e.,

$$\tilde{g}(\zeta) = \sup_{\theta \in \Theta} \{\theta^\top \zeta - \tilde{g}^*(\theta)\}, \forall \zeta \in \mathbb{R}^M,$$

where the conjugate function $\tilde{g}^*(\theta) := \sup_{\zeta \in \mathbb{R}^M} \{\theta^\top \zeta - \tilde{g}(\zeta)\}$ and $\Theta := \{\theta | \tilde{g}^*(\theta) < \infty\}$.

Claim 3: $\Theta = \text{conv}\{B^\top \pi | \pi \in \tilde{V}\}$, i.e., the convex hull of $\{B^\top \pi | \pi \in \tilde{V}\}$.

Proof: (1) Prove that $\text{conv}\{B^\top \pi | \pi \in \tilde{V}\} \subset \Theta$.

For any $\theta \in \text{conv}\{B^\top \pi | \pi \in \tilde{V}\}$, there exist $\pi_i \in \tilde{V}$ and $\lambda_i, i \in \mathcal{I}$ subject to $\lambda_i \geq 0, i \in \mathcal{I}, \sum_{i \in \mathcal{I}} \lambda_i = 1$ and $\theta = \sum_{i \in \mathcal{I}} \lambda_i B^\top \pi_i$, so

$$\begin{aligned} \tilde{g}(\zeta) &= \max_{\pi \in \tilde{V}} \{\pi^\top B \zeta + \pi^\top D\} \\ &= \sum_{i \in \mathcal{I}} \lambda_i \max_{\pi \in \tilde{V}} \{\pi^\top B \zeta + \pi^\top D\} \\ &\geq \sum_{i \in \mathcal{I}} \lambda_i (\pi_i^\top B \zeta + \pi_i^\top D) \\ &= \theta^\top \zeta + \sum_{i \in \mathcal{I}} \lambda_i \pi_i^\top D, \end{aligned}$$

and then

$$\sup_{\zeta \in \mathbb{R}^M} \{\theta^\top \zeta - \tilde{g}(\zeta)\} \leq - \sum_{i \in \mathcal{I}} \lambda_i \pi_i^\top D \leq \max_{\pi \in \tilde{V}} |\pi^\top D| < +\infty,$$

which means $\theta \in \Theta$. Thus, $\text{conv}\{B^\top \pi | \pi \in \tilde{V}\} \subset \Theta$.

(2) Prove that $\Theta \subset \text{conv}\{B^\top \pi | \pi \in \tilde{V}\}$.

Assume $\theta \notin \text{conv}\{B^\top \pi | \pi \in \tilde{V}\}$. Since \tilde{V} is a finite set, $\text{conv}\{B^\top \pi | \pi \in \tilde{V}\}$ is closed and convex. Then θ and $\text{conv}\{B^\top \pi | \pi \in \tilde{V}\}$ can be strictly separated [32], i.e., there are vector $a \neq 0$ and constant $\varepsilon > 0$ such that $\theta^\top a - \varepsilon \geq \pi^\top B a, \forall \pi \in \tilde{V}$. Then for any $\lambda > 0$, we have

$$\begin{aligned} \tilde{g}(\lambda a) &= \max_{\pi \in \tilde{V}} \{\pi^\top B(\lambda a) + \pi^\top D\} \\ &\leq \max_{\pi \in \tilde{V}} \{\lambda(\theta^\top a - \varepsilon) + \pi^\top D\} \\ &= \lambda(\theta^\top a - \varepsilon) + \max_{\pi \in \tilde{V}} \{\pi^\top D\}, \end{aligned}$$

then

$$\begin{aligned} \theta^\top(\lambda a) - \tilde{g}(\lambda a) &\geq \theta^\top(\lambda a) - \lambda(\theta^\top a - \varepsilon) - \max_{\pi \in \tilde{V}} \{\pi^\top D\} \\ &= \lambda \varepsilon - \max_{\pi \in \tilde{V}} \{\pi^\top D\} \rightarrow +\infty (\lambda \rightarrow +\infty), \end{aligned}$$

which means $\theta \notin \Theta$. Thus, $\Theta \subset \text{conv}\{B^\top \pi | \pi \in \tilde{V}\}$. \square

Claim 4: $L_i^{WE} = \sup_{\theta \in \Theta} \|\theta_i^W\|_\infty = \max_{\pi \in \tilde{V}} \|(B^\top \pi)_i^W\|_\infty$, where $(B^\top \pi)_i^W$ denotes the projection of $(B^\top \pi)$ to the component corresponding to the wind farm at bus i .

Proof: $\sup_{\theta \in \Theta} \|\theta_i^W\|_\infty = \max_{\pi \in \tilde{V}} \|(B^\top \pi)_i^W\|_\infty$ directly follows from $\Theta = \text{conv}\{B^\top \pi | \pi \in \tilde{V}\}$ and that \tilde{V} is finite. We prove $L_i^{WE} = \max_{\pi \in \tilde{V}} \|(B^\top \pi)_i^W\|_\infty$.

(1) Prove that $L_i^{WE} \geq \max_{\pi \in \tilde{V}} \|(B^\top \pi)_i^W\|_\infty$.

There is a $\pi_0 \in \tilde{V}$ such that

$$\|(B^\top \pi_0)_i^W\|_\infty = \max_{\pi \in \tilde{V}} \|(B^\top \pi)_i^W\|_\infty.$$

According to the definition of \tilde{V} , there is an open set $U \subset \Xi_{\pi_0} \subset \Xi^E$. For $\zeta, \check{\zeta} \in U$, $g^E(\zeta) = \tilde{g}(\zeta) = \pi_0^\top B \zeta + \pi_0^\top D$ and $g^E(\check{\zeta}) = \tilde{g}(\check{\zeta}) = \pi_0^\top B \check{\zeta} + \pi_0^\top D$. Since U is open, we can choose ζ and $\check{\zeta}$ so that $\zeta^D = \check{\zeta}^D$, $\zeta_j^W = \check{\zeta}_j^W$ for any $j \neq i$ and

$$|g^E(\zeta) - g^E(\check{\zeta})| = |\pi_0^\top B(\zeta - \check{\zeta})|$$

$$\begin{aligned}
&= \|(B^\top \pi_0)_i^W\|_\infty \|(\zeta - \check{\zeta})_i^W\|_1 \\
&= \|(B^\top \pi_0)_i^W\|_\infty \|\zeta - \check{\zeta}\|_1,
\end{aligned}$$

due to the property of dual norm. Then by the definition of L_i^{WE} , we have $L_i^{WE} \geq \|(B^\top \pi_0)_i^W\|_\infty = \max_{\pi \in \tilde{\mathcal{V}}} \|(B^\top \pi)_i^W\|_\infty$.

(2) Prove that $L_i^{WE} \leq \max_{\pi \in \tilde{\mathcal{V}}} \|(B^\top \pi)_i^W\|_\infty$.

For arbitrary $\zeta, \check{\zeta} \in \Xi^E$ subject to $\zeta^D = \check{\zeta}^D$ and $\zeta_j^W = \check{\zeta}_j^W$ for any $j \neq i$, there are π_0 and $\check{\pi}_0$ so that

$$\begin{aligned}
g^E(\zeta) &= \tilde{g}(\zeta) = \pi_0^\top B \zeta + \pi_0^\top D \geq \check{\pi}_0^\top B \zeta + \check{\pi}_0^\top D, \\
g^E(\check{\zeta}) &= \tilde{g}(\check{\zeta}) = \check{\pi}_0^\top B \check{\zeta} + \check{\pi}_0^\top D \geq \pi_0^\top B \check{\zeta} + \pi_0^\top D,
\end{aligned}$$

so

$$\check{\pi}_0^\top B(\zeta - \check{\zeta}) \leq g^E(\zeta) - g^E(\check{\zeta}) \leq \pi_0^\top B(\zeta - \check{\zeta}),$$

and then

$$\begin{aligned}
|g^E(\zeta) - g^E(\check{\zeta})| &\leq \max_{\pi \in \tilde{\mathcal{V}}} |\pi^\top B(\zeta - \check{\zeta})| \\
&\leq \max_{\pi \in \tilde{\mathcal{V}}} \|(B^\top \pi)_i^W\|_\infty \cdot \|\zeta - \check{\zeta}\|_1.
\end{aligned}$$

Since ζ and $\check{\zeta}$ are arbitrary, we have $L_i^{WE} \leq \max_{\pi \in \tilde{\mathcal{V}}} \|(B^\top \pi)_i^W\|_\infty$. □

Similarly, $L^{DE} = \sup_{\theta \in \Theta} \|\theta^D\|_\infty = \max_{\pi \in \tilde{\mathcal{V}}} \|(B^\top \pi)^D\|_\infty$.

Remark: The fuel cost function g^N can be handled in a similar way when the dimension of Ξ^N is M .

Appendix A.2. Distributionally Robust Expectation

The proof in this subsection is analogous to that in [38].

By the definition of $\mathcal{B}^E(\varepsilon^E)$ in (12), the distributionally robust expectation is

$$\begin{aligned}
&\sup_{\mathbb{P} \in \mathcal{B}^E(\varepsilon^E)} \mathbb{E}_{\mathbb{P}}[g^E(\zeta)] = \sup_{\mathbb{P} \in \mathcal{B}^E(\varepsilon^E)} \mathbb{E}_{\mathbb{P}}[\tilde{g}(\zeta)] \\
&= \left\{ \begin{array}{l} \sup \int_{\Xi_i^{WE} \times \Xi^D} \tilde{g}(\zeta) \left(\frac{1}{|S^E|} \sum_{n \in S^E} \left(\bigotimes_{i \in S^B} \mathbb{P}_{i,n}^W \right) \otimes \mathbb{P}_n^D \right) (d\zeta) \\ \text{s.t. } \mathbb{P}_{i,n}^W \in \mathcal{M}(\Xi_i^{WE}), \Pi_i^W = \frac{1}{|S^E|} \sum_{n \in S^E} \mathbb{P}_{i,n}^W \otimes \delta_{\zeta_{i,n}^W} \\ \int_{(\Xi_i^{WE})^2} \|\zeta_i^W - \check{\zeta}_i^W\|_1 \Pi_i^W(d\zeta_i^W, d\check{\zeta}_i^W) \leq \varepsilon_i^{WE} x_i^W \\ \mathbb{P}_n^D \in \mathcal{M}(\Xi^{DE}), \Pi^D = \frac{1}{|S^E|} \sum_{n \in S^E} \mathbb{P}_n^D \otimes \delta_{\zeta_n^D} \\ \int_{(\Xi^{DE})^2} \|\zeta^D - \check{\zeta}^D\|_1 \Pi^D(d\zeta^D, d\check{\zeta}^D) \leq \varepsilon^{DE} \end{array} \right.
\end{aligned}$$

$$= \left\{ \begin{array}{l} \sup \frac{1}{|S^E|} \sum_{n \in S^E} \int_{\Xi^E} \tilde{g}(\zeta) \mathbb{P}_n(d\zeta) \\ \text{s.t. } \mathbb{P}_{i,n}^W \in \mathcal{M}(\Xi_i^{WE}), \mathbb{P}_n^D \in \mathcal{M}(\Xi^{DE}) \\ \mathbb{P}_n = \left(\bigotimes_{i \in S^B} \mathbb{P}_{i,n}^W \right) \otimes \mathbb{P}_n^D \\ \frac{1}{|S^E|} \sum_{n \in S^E} \int_{\Xi_i^{WE}} \|\zeta_i^W - \hat{\zeta}_{i,n}^W\|_1 \mathbb{P}_{i,n}^W(d\zeta_i^W) \leq \varepsilon_i^{WE} x_i^W \\ \frac{1}{|S^E|} \sum_{n \in S^E} \int_{\Xi^{DE}} \|\zeta^D - \hat{\zeta}_n^D\|_1 \mathbb{P}_n^D(d\zeta^D) \leq \varepsilon^{DE} \end{array} \right. , \quad (\text{A.7})$$

where $\Xi^E = (\times_{i \in S^B} \Xi_i^{WE}) \times \Xi^{DE}$; (A.7) follows from the linearity of expectation and the definitions of Dirac distribution and joint distribution.

Using the duality technique, we have

$$= \left\{ \begin{array}{l} \sup_{\mathbb{P} \in \mathcal{B}^E(\varepsilon^E)} \mathbb{E}_{\mathbb{P}}[g^E(\zeta)] \\ \sup_{\mathbb{P}} \inf_{\lambda} \frac{1}{|S^E|} \sum_{n \in S^E} \int_{\Xi^E} \tilde{g}(\zeta) \mathbb{P}_n(d\zeta) + \sum_{i \in S^B} \lambda_i^W \{ \varepsilon_i^{WE} x_i^W \\ - \frac{1}{|S^E|} \sum_{n \in S^E} \int_{\Xi_i^{WE}} \|\zeta_i^W - \hat{\zeta}_{i,n}^W\|_1 \mathbb{P}_{i,n}^W(d\zeta_i^W) \} \\ + \lambda^D \{ \varepsilon^{DE} - \frac{1}{|S^E|} \sum_{n \in S^E} \int_{\Xi^{DE}} \|\zeta^D - \hat{\zeta}_n^D\|_1 \mathbb{P}_n^D(d\zeta^D) \} \\ \text{s.t. } \mathbb{P}_{i,n}^W \in \mathcal{M}(\Xi_i^{WE}), \mathbb{P}_n^D \in \mathcal{M}(\Xi^{DE}), \lambda_i^W \geq 0, \lambda^D \geq 0 \\ \mathbb{P}_n = \left(\bigotimes_{i \in S^B} \mathbb{P}_{i,n}^W \right) \otimes \mathbb{P}_n^D \end{array} \right. \quad (\text{A.8})$$

$$= \left\{ \begin{array}{l} \inf_{\lambda} \sup_{\mathbb{P}} \sum_{i \in S^B} \lambda_i^W \varepsilon_i^{WE} x_i^W + \lambda^D \varepsilon^{DE} \\ + \frac{1}{|S^E|} \sum_{n \in S^E} \left(\int_{\Xi^E} \tilde{g}(\zeta) \mathbb{P}_n(d\zeta) \right. \\ - \sum_{i \in S^B} \lambda_i^W \int_{\Xi_i^{WE}} \|\zeta_i^W - \hat{\zeta}_{i,n}^W\|_1 \mathbb{P}_{i,n}^W(d\zeta_i^W) \\ \left. - \lambda^D \int_{\Xi^{DE}} \|\zeta^D - \hat{\zeta}_n^D\|_1 \mathbb{P}_n^D(d\zeta^D) \right) \\ \text{s.t. } \mathbb{P}_{i,n}^W \in \mathcal{M}(\Xi_i^{WE}), \mathbb{P}_n^D \in \mathcal{M}(\Xi^{DE}), \lambda_i^W \geq 0, \lambda^D \geq 0 \\ \mathbb{P}_n = \left(\bigotimes_{i \in S^B} \mathbb{P}_{i,n}^W \right) \otimes \mathbb{P}_n^D \end{array} \right. \quad (\text{A.9})$$

$$= \left\{ \begin{array}{l} \inf_{\lambda} \sum_{i \in S^B} \lambda_i^W \varepsilon_i^{WE} x_i^W + \lambda^D \varepsilon^{DE} \\ + \frac{1}{|S^E|} \sum_{n \in S^E} \sup_{\zeta \in \Xi^E} \{ \tilde{g}(\zeta) - \sum_{i \in S^B} \lambda_i^W \|\zeta_i^W - \hat{\zeta}_{i,n}^W\|_1 \\ - \lambda^D \|\zeta^D - \hat{\zeta}_n^D\|_1 \} \\ \text{s.t. } \lambda_i^W \geq 0, \lambda^D \geq 0 \end{array} \right. \quad (\text{A.10})$$

From (A.8) to (A.9), the “ \leq ” direction uses the max-min inequality, and the opposite direction follows from the strong duality result of moment problems [39]. The Dirac distribution δ_ζ for $\zeta \in \Xi^E$ can be regarded as a product of Dirac distributions on Ξ_i^{WE} and Ξ^{DE} , so (A.10) holds.

Using $\tilde{g} = \tilde{g}^{**}$, we have

$$\begin{aligned}
& \sup_{\zeta \in \Xi^E} \{ \tilde{g}(\zeta) - \sum_{i \in S^B} \lambda_i^W \|\zeta_i^W - \hat{\zeta}_{i,n}^W\|_1 - \lambda^D \|\zeta^D - \hat{\zeta}_n^D\|_1 \} \\
&= \sup_{\zeta \in \Xi^E} \sup_{\theta \in \Theta} \{ \theta^\top \zeta - \tilde{g}^*(\theta) - \sum_{i \in S^B} \lambda_i^W \|\zeta_i^W - \hat{\zeta}_{i,n}^W\|_1 \\
&\quad - \lambda^D \|\zeta^D - \hat{\zeta}_n^D\|_1 \} \\
&= \sup_{\zeta \in \Xi^E} \sup_{\theta \in \Theta} \inf_{\mu: \|\mu_i^W\|_\infty \leq \lambda_i^W, \|\mu^D\|_\infty \leq \lambda^D} \{ \theta^\top \zeta - \tilde{g}^*(\theta) \\
&\quad + \sum_{i \in S^B} ((\mu_i^W)^\top \zeta_i^W - (\mu_i^W)^\top \hat{\zeta}_{i,n}^W) + (\mu^D)^\top \zeta^D - (\mu^D)^\top \hat{\zeta}_n^D \} \tag{A.11}
\end{aligned}$$

$$\begin{aligned}
&= \sup_{\zeta \in \Xi^E} \sup_{\theta \in \Theta} \inf_{\mu: \|\mu_i^W\|_\infty \leq \lambda_i^W, \|\mu^D\|_\infty \leq \lambda^D} \{ (\theta + \mu)^\top \zeta - \tilde{g}^*(\theta) - \mu^\top \hat{\zeta}_n \} \\
&= \sup_{\theta \in \Theta} \inf_{\mu: \|\mu_i^W\|_\infty \leq \lambda_i^W, \|\mu^D\|_\infty \leq \lambda^D} \sup_{\zeta \in \Xi^E} \{ (\theta + \mu)^\top \zeta - \tilde{g}^*(\theta) - \mu^\top \hat{\zeta}_n \} \tag{A.12}
\end{aligned}$$

$$\leq \sup_{\theta \in \Theta} \inf_{\mu: \|\mu_i^W\|_\infty \leq \lambda_i^W, \|\mu^D\|_\infty \leq \lambda^D} \sup_{\zeta \in \mathbb{R}^M} \{ (\theta + \mu)^\top \zeta - \tilde{g}^*(\theta) - \mu^\top \hat{\zeta}_n \}, \tag{A.13}$$

where (A.11) follows from the property of dual norm; (A.12) is a consequence of the minimax theorem [37]. Since

$$\sup_{\zeta \in \mathbb{R}^M} \{ (\theta + \mu)^\top \zeta \} = \begin{cases} 0, & \text{if } \mu = -\theta, \\ +\infty, & \text{otherwise,} \end{cases}$$

we have (A.13) = $\sup_{\theta \in \Theta} \{ -\tilde{g}^*(\theta) + \theta^\top \hat{\zeta}_n \} = \tilde{g}(\hat{\zeta}_n) = g^E(\hat{\zeta}_n)$ if $\|\theta_i^W\|_\infty \leq \lambda_i^W$ and $\|\theta^D\|_\infty \leq \lambda^D, \forall \theta \in \Theta$; otherwise, (A.13) = $+\infty$. Therefore,

$$\begin{aligned}
& \sup_{\mathbb{P} \in \mathcal{B}^E(\mathcal{E}^E)} \mathbb{E}_{\mathbb{P}}[g^E(\zeta)] \\
&\leq \begin{cases} \inf_{\lambda} \sum_{i \in S^B} \lambda_i^W \varepsilon_i^{WE} x_i^W + \lambda^D \varepsilon^{DE} \\ \quad + \frac{1}{|S^E|} \sum_{n \in S^E} \sup_{\zeta \in \mathbb{R}^M} \{ \tilde{g}(\zeta) - \sum_{i \in S^B} \lambda_i^W \|\zeta_i^W - \hat{\zeta}_{i,n}^W\|_1 \\ \quad - \lambda^D \|\zeta^D - \hat{\zeta}_n^D\|_1 \} \\ \text{s.t. } \lambda_i^W \geq 0, \lambda^D \geq 0 \end{cases} \\
&= \sum_{i \in S^B} \left(\sup_{\theta \in \Theta} \|\theta_i^W\|_\infty \right) \varepsilon_i^{WE} x_i^W \\
&\quad + \left(\sup_{\theta \in \Theta} \|\theta^D\|_\infty \right) \varepsilon^{DE} + \frac{1}{|S^E|} \sum_{n \in S^E} g^E(\hat{\zeta}_n) \\
&= \sum_{i \in S^B} L_i^{WE} \varepsilon_i^{WE} x_i^W + L^{DE} \varepsilon^{DE} + \mathbb{E}_{\mathbb{P}_0^E}[g^E(\zeta)],
\end{aligned}$$

by Claim 4. This completes the proof.

Appendix B. Calculating Lipschitz Constants

The methods of calculating Lipschitz constants are different for g^E and g^N since their domains are defined in different ways.

Appendix B.1. Lipschitz Constants of the Load Shedding Function

The definition of load shedding function in (9) can be written in the following compact form:

$$g^E(x, \zeta) := \min_y C^\top y \quad (\text{B.1a})$$

$$\text{s.t. } A_1 y \geq B_1 x + B_2 \zeta + B_3 \quad (\text{B.1b})$$

$$A_2 y = B_4 x + B_5 \zeta + B_6, \quad (\text{B.1c})$$

where $A_1, A_2, B_1, B_2, B_3, B_4, B_5, B_6$, and C are coefficient matrices or vectors; y represents the operation variables. The dual problem of (B.1) is

$$\max_{\lambda, \mu} (B_1 x + B_2 \zeta + B_3)^\top \lambda + (B_4 x + B_5 \zeta + B_6)^\top \mu \quad (\text{B.2a})$$

$$\text{s.t. } A_1^\top \lambda + A_2^\top \mu = C, \lambda \geq 0. \quad (\text{B.2b})$$

Because the LP problem (B.1) has a finite optimal value for any $x \in \mathcal{X}$ and $\zeta \in \Xi^E$, the strong duality holds [32]. Then for dual optimal solution (λ, μ) , we have

$$\begin{aligned} g^E(x, \zeta) &= (B_1 x + B_2 \zeta + B_3)^\top \lambda + (B_4 x + B_5 \zeta + B_6)^\top \mu \\ &= (B_2^\top \lambda + B_5^\top \mu)^\top \zeta + (B_1 x + B_3)^\top \lambda + (B_4 x + B_6)^\top \mu, \end{aligned}$$

which shows that the value of $B_2^\top \lambda + B_5^\top \mu$ reflects how $g^E(x, \zeta)$ changes as ζ varies.

For fixed $x \in \mathcal{X}$, in order to find a Lipschitz constant $\tilde{L}_i^{WE}(x)$, we solve the following optimization problem.

$$\max_{\zeta, y, \lambda, \mu, \gamma} -\gamma_a \quad (\text{B.3a})$$

$$\text{s.t. } \zeta \in \Xi^E, \gamma = B_2^\top \lambda + B_5^\top \mu \quad (\text{B.3b})$$

$$0 \leq A_1 y - B_1 x - B_2 \zeta - B_3 \perp \lambda \geq 0 \quad (\text{B.3c})$$

$$A_2 y = B_4 x + B_5 \zeta + B_6, A_1^\top \lambda + A_2^\top \mu = C, \quad (\text{B.3d})$$

where the decision variables are ζ, y, λ, μ , and γ . In (B.3a), γ_a represents a component corresponding to ζ_i^W . Any such component works because all $t \in \{1, 2, \dots, T\}$ lead to equivalent problems, which can be observed from (9) and the power system operation constraints. Since larger wind power output results in smaller load shedding, $-\gamma_a$ is maximized in (B.3a). Constraints (B.3c) and (B.3d) form the KKT condition of problem (B.1), where (B.3c) can be linearized by the big-M technique [40], so that (B.3) is transformed into an MILP problem. It can also be solved directly as a bilinear program using solvers. Its optimal value or any upper bound can be the desired $\tilde{L}_i^{WE}(x)$.

We can also find a uniform bound \tilde{L}_i^{WE} so that $\tilde{L}_i^{WE} \geq \tilde{L}_i^{WE}(x), \forall x \in \mathcal{X}$ by the optimization problem below.

$$\max_{x, \zeta, y, \lambda, \mu, \gamma} -\gamma_a \quad (\text{B.4a})$$

$$\text{s.t. } x \in \mathcal{X}, (\text{B.3b}) - (\text{B.3d}), \quad (\text{B.4b})$$

which is modified from (B.3) by allowing x to vary within \mathcal{X} . This problem can still be either directly solved as a bilinear program or transformed into an MILP problem and then solved.

Appendix B.2. Lipschitz Constants of the Fuel Cost Function

The definition of the fuel cost function $g^N(x, \zeta)$ can also be written in the form of (B.1), and so is the dual problem (B.2). When x is fixed, $g^N(x, \zeta)$ is a convex and piecewise linear function of ζ . According to the relation of Lipschitz continuity and local Lipschitz continuity [41], the maximum local Lipschitz constant at $\hat{\zeta}_n, n \in S^N$ is also a Lipschitz constant on Ξ^N . Therefore, solve the dual problem (B.2) at each $\hat{\zeta}_n, n \in S^N$ to find the dual optimal solutions $(\hat{\lambda}_n(x), \hat{\mu}_n(x)), n \in S^N$, where x emphasizes that they are dependent on x . Then calculate $-(B_2^\top \hat{\lambda}_n(x) + B_5^\top \hat{\mu}_n(x))$, extract the component corresponding to ζ_i^W , and denote it by $\hat{\gamma}_{i,n}^W(x)$. Note that $\hat{\gamma}_{i,n}^W(x) = (\hat{\gamma}_{i,t,n}^W(x); t \in S^T)$ is a vector with T dimensions. Then $\tilde{L}_i^{WN}(x)$ can be estimated by $\max_{n \in S^N} \max_{t \in S^T} \hat{\gamma}_{i,t,n}^W(x)$. The Lipschitz constant $\tilde{L}^{DN}(x)$ can be estimated in a similar way.

References

- [1] X. Wu, Z. Tian, J. Guo, A review of the theoretical research and practical progress of carbon neutrality, *Sustainable Operations and Computers* 3 (2022) 54–66.
- [2] C. Opathella, A. Elkasrawy, A. A. Mohamed, B. Venkatesh, Milp formulation for generation and storage asset sizing and siting for reliability constrained system planning, *International Journal of Electrical Power & Energy Systems* 116 (2020) 105529.
- [3] T. Zhao, N. Raghunathan, A. Yogarathnam, M. Yue, P. B. Luh, A scalable planning framework of energy storage systems under frequency dynamics constraints, *International Journal of Electrical Power & Energy Systems* 145 (2023) 108693.
- [4] X. Zhang, Z. Wang, H. Liao, Z. Zhou, X. Ma, X. Yin, Z. Wang, Y. Liu, Z. Lu, G. Lv, Optimal capacity planning and operation of shared energy storage system for large-scale photovoltaic integrated 5g base stations, *International Journal of Electrical Power & Energy Systems* 147 (2023) 108816.
- [5] W. Yin, Y. Li, J. Hou, M. Miao, Y. Hou, Coordinated planning of wind power generation and energy storage with decision-dependent uncertainty induced by spatial correlation, *IEEE Systems Journal* (2022) 1–12 doi : 10 . 1109 / JSYST . 2022 . 3196706.
- [6] S. Dehghan, N. Amjady, P. Aristidou, A robust coordinated expansion planning model for wind farm-integrated power systems with flexibility sources using affine policies, *IEEE Systems Journal* 14 (3) (2019) 4110–4118.
- [7] C. Yan, X. Geng, Z. Bie, L. Xie, Two-stage robust energy storage planning with probabilistic guarantees: A data-driven approach, *Applied Energy* 313 (2022) 118623.
- [8] B. Li, R. Jiang, J. L. Mathieu, Integrating unimodality into distributionally robust optimal power flow, *Top* 30 (3) (2022) 594–617.
- [9] A. Esteban-Pérez, J. M. Morales, Distributionally robust optimal power flow with contextual information, *European Journal of Operational Research* 306 (3) (2023) 1047–1058.
- [10] H. Li, H. Liu, J. Ma, D. Li, W. Zhang, Distributionally robust optimal dispatching method of integrated electricity and heating system based on improved wasserstein metric, *International Journal of Electrical Power & Energy Systems* 151 (2023) 109120.
- [11] F. Pourahmadi, J. Kazempour, Distributionally robust generation expansion planning with unimodality and risk constraints, *IEEE Transactions on Power Systems* 36 (5) (2021) 4281–4295.

- [12] J. Le, X. Liao, L. Zhang, T. Mao, Distributionally robust chance constrained planning model for energy storage plants based on kullback–leibler divergence, *Energy Reports* 7 (2021) 5203–5213.
- [13] B. Chen, T. Liu, X. Liu, C. He, L. Nan, L. Wu, X. Su, J. Zhang, A wasserstein distance-based distributionally robust chance-constrained clustered generation expansion planning considering flexible resource investments, *IEEE Transactions on Power Systems* (2022).
- [14] Z. Ren, H. Li, W. Li, X. Zhao, Y. Sun, T. Li, F. Jiang, Reliability evaluation of tidal current farm integrated generation systems considering wake effects, *IEEE Access* 6 (2018) 52616–52624.
- [15] A. P. Gupta, A. Mitra, A. Mohapatra, S. N. Singh, A multi-machine equivalent model of a wind farm considering lvr characteristic and wake effect, *IEEE Transactions on Sustainable Energy* 13 (3) (2022) 1396–1407.
- [16] B. He, H. Zhao, G. Liang, J. Zhao, J. Qiu, Z. Y. Dong, Ensemble-based deep reinforcement learning for robust cooperative wind farm control, *International Journal of Electrical Power & Energy Systems* 143 (2022) 108406.
- [17] W. Yin, X. Peng, Y. Hou, A decision-dependent stochastic approach for wind farm maintenance scheduling considering wake effect, in: 2020 IEEE PES Innovative Smart Grid Technologies Europe (ISGT-Europe), IEEE, 2020, pp. 814–818.
- [18] X. Gao, H. Yang, L. Lu, Optimization of wind turbine layout position in a wind farm using a newly-developed two-dimensional wake model, *Applied Energy* 174 (2016) 192–200.
- [19] M. Lerch, M. De-Prada-Gil, C. Molins, A metaheuristic optimization model for the inter-array layout planning of floating offshore wind farms, *International Journal of Electrical Power & Energy Systems* 131 (2021) 107128.
- [20] F. Bai, X. Ju, S. Wang, W. Zhou, F. Liu, Wind farm layout optimization using adaptive evolutionary algorithm with monte carlo tree search reinforcement learning, *Energy Conversion and Management* 252 (2022) 115047.
- [21] D. Cazzaro, A. Trivella, F. Corman, D. Pisinger, Multi-scale optimization of the design of offshore wind farms, *Applied energy* 314 (2022) 118830.
- [22] L. Xiong, S. Yang, S. Huang, D. He, P. Li, M. W. Khan, J. Wang, Optimal allocation of energy storage system in dfig wind farms for frequency support considering wake effect, *IEEE Transactions on Power Systems* 37 (3) (2021) 2097–2112.
- [23] O. Sadeghian, A. Oshnoei, M. Tarafdar-Hagh, M. Kheradmandi, A clustering-based approach for wind farm placement in radial distribution systems considering wake effect and a time-acceleration constraint, *IEEE Systems Journal* 15 (1) (2020) 985–995.
- [24] J. S. González, M. B. Payán, J. M. R. Santos, F. González-Longatt, A review and recent developments in the optimal wind-turbine micro-siting problem, *Renewable and Sustainable Energy Reviews* 30 (2014) 133–144.
- [25] A. E. Feijoo, J. Cidras, Modeling of wind farms in the load flow analysis, *IEEE transactions on power systems* 15 (1) (2000) 110–115.
- [26] D. Villanueva, J. L. Pazos, A. Feijoo, Probabilistic load flow including wind power generation, *IEEE Transactions on Power Systems* 26 (3) (2011) 1659–1667.

- [27] M. Herceg, M. Kvasnica, C. Jones, M. Morari, Multi-Parametric Toolbox 3.0, in: Proc. of the European Control Conference, Zürich, Switzerland, 2013, pp. 502–510, <http://control.ee.ethz.ch/~mpt>.
- [28] R. Xie, W. Wei, M. Li, Z. Dong, S. Mei, Sizing capacities of renewable generation, transmission, and energy storage for low-carbon power systems: A distributionally robust optimization approach, *Energy* 263 (2023) 125653.
- [29] L. V. Kantorovich, S. Rubinshtein, On a space of totally additive functions, *Vestnik of the St. Petersburg University: Mathematics* 13 (7) (1958) 52–59.
- [30] N. Fournier, A. Guillin, On the rate of convergence in wasserstein distance of the empirical measure, *Probability Theory and Related Fields* 162 (2015) 707–738.
- [31] F. Luo, S. Mehrotra, Distributionally robust optimization with decision dependent ambiguity sets, *Optimization Letters* 14 (2020) 2565–2594.
- [32] S. Boyd, L. Vandenberghe, *Convex optimization*, Cambridge university press, 2004.
- [33] K. M. Miettinen, *Nonlinear Multiobjective Optimization*, Kluwer Academic Publishers, 1999.
- [34] R. Xie, Wind farm planning considering wake effect, <https://github.com/xieruijx/wind-farm-planning-considering-wake-effect> (2022).
- [35] K. Yang, G. Kwak, K. Cho, J. Huh, Wind farm layout optimization for wake effect uniformity, *Energy* 183 (2019) 983–995.
- [36] I. Staffell, S. Pfenninger, Using bias-corrected reanalysis to simulate current and future wind power output, *Energy* 114 (2016) 1224–1239.
- [37] D. Bertsekas, *Convex optimization theory*, Vol. 1, Athena Scientific, 2009.
- [38] P. M. Esfahani, D. Kuhn, Data-driven distributionally robust optimization using the wasserstein metric: performance guarantees and tractable reformulations, *Mathematical Programming* 171 (2018) 115–166.
- [39] A. Shapiro, On duality theory of conic linear problems, *Semi-Infinite Programming: Recent Advances* (2001) 135–165.
- [40] S. Pineda, J. M. Morales, Solving linear bilevel problems using big-ms: not all that glitters is gold, *IEEE Transactions on Power Systems* 34 (3) (2019) 2469–2471.
- [41] B. T. Nguyen, P. D. Khanh, Lipschitz continuity of convex functions, *Applied Mathematics & Optimization* 84 (2021) 1623–1640.